(12) INTERNATIONAL APPLICATION PUBLISHED UNDER THE PATENT COOPERATION TREATY (PCT)

(19) World Intellectual Property Organization
International Bureau

(43) International Publication Date
15 June 2017 (15.06.2017)

WIPO | PCT

(10) International Publication Number
WO 2017/100442 A1

(51) International Patent Classification:
C12Q 1/68 (2006.01)

(21) International Application Number:
PCT/US2016/065607

(22) International Filing Date:
8 December 2016 (08.12.2016)

(25) Filing Language: English

(26) Publication Language: English

(30) Priority Data:
62/264,818 8 December 2015 (08.12.2015) US
62/287,799 27 January 2016 (27.01.2016) US

(71) Applicant: **SELUX DIAGNOSTICS, INC.** [US/US]; Suite B-14302, One Kendall Square, Cambridge, MA 02139 (US).

(72) Inventors: **STERN, Eric**; One Kendall Square, Suite B-14302, Cambridge, MA 02139 (US). **FLYER, Alec, Nathanson**; One Kendall Square, Suite B-14302, Cambridge, MA 02139 (US).

(74) Agents: **CHEN, Fangli** et al.; Proskauer Rose LLP, One International Place, Boston, MA 02110 (US).

(81) Designated States *(unless otherwise indicated, for every kind of national protection available)*: AE, AG, AL, AM, AO, AT, AU, AZ, BA, BB, BG, BH, BN, BR, BW, BY, BZ, CA, CH, CL, CN, CO, CR, CU, CZ, DE, DJ, DK, DM, DO, DZ, EC, EE, EG, ES, FI, GB, GD, GE, GH, GM, GT, HN, HR, HU, ID, IL, IN, IR, IS, JP, KE, KG, KH, KN, KP, KR, KW, KZ, LA, LC, LK, LR, LS, LU, LY, MA, MD, ME, MG, MK, MN, MW, MX, MY, MZ, NA, NG, NI, NO, NZ, OM, PA, PE, PG, PH, PL, PT, QA, RO, RS, RU, RW, SA, SC, SD, SE, SG, SK, SL, SM, ST, SV, SY, TH, TJ, TM, TN, TR, TT, TZ, UA, UG, US, UZ, VC, VN, ZA, ZM, ZW.

(84) Designated States *(unless otherwise indicated, for every kind of regional protection available)*: ARIPO (BW, GH, GM, KE, LR, LS, MW, MZ, NA, RW, SD, SL, ST, SZ, TZ, UG, ZM, ZW), Eurasian (AM, AZ, BY, KG, KZ, RU, TJ, TM), European (AL, AT, BE, BG, CH, CY, CZ, DE, DK, EE, ES, FI, FR, GB, GR, HR, HU, IE, IS, IT, LT, LU, LV, MC, MK, MT, NL, NO, PL, PT, RO, RS, SE, SI, SK, SM, TR), OAPI (BF, BJ, CF, CG, CI, CM, GA, GN, GQ, GW, KM, ML, MR, NE, SN, TD, TG).

Declarations under Rule 4.17:

— *as to applicant's entitlement to apply for and be granted a patent (Rule 4.17(ii))*

— *as to the applicant's entitlement to claim the priority of the earlier application (Rule 4.17(iii))*

Published:

— *with international search report (Art. 21(3))*

— *with sequence listing part of description (Rule 5.2(a))*

(54) Title: NANOPARTICLE AMPLIFIERS AND USES THEREOF

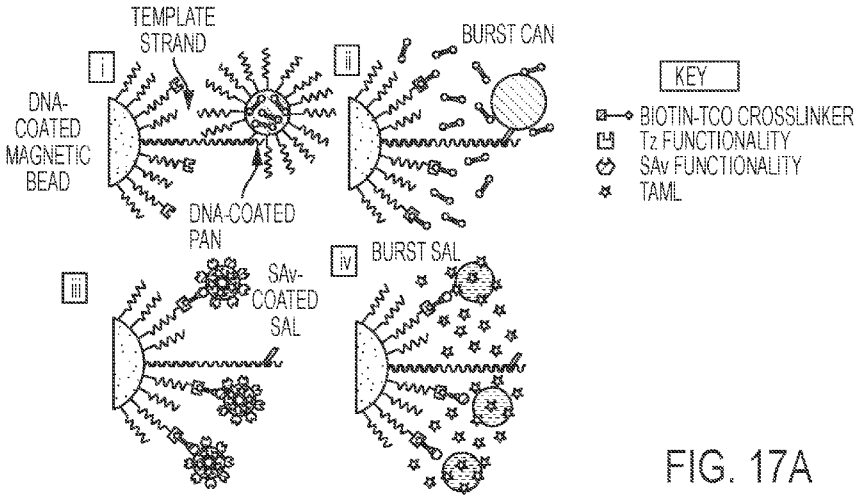


FIG. 17A

(57) Abstract: Described herein are nanoparticle synthetic amplifier labels ("SAL") that can permit existing microplate readers to quantify proteins with increased sensitivity versus ELISAs. Such labels can be used in immunoassays as well as DNA and RNA assays, with sensitivities approaching quantitative PCR.

WO 2017/100442 A1

Nanoparticle amplifiers and uses thereof

CROSS-REFERENCE TO RELATED APPLICATIONS

[0001] The present application claims benefit of U.S. Provisional Application Nos. 62/264,818, filed December 8, 2015, and 62/287,799, filed January 27, 2016, each of which is incorporated by reference in its entirety.

SEQUENCE LISTING

[0002] The instant application contains a Sequence Listing which has been submitted electronically in ASCII format and is hereby incorporated by reference in its entirety. Said ASCII copy, created on December 6, 2016, is named "SLX-010WO Sequence Listing_ST25.txt" and is 2,597 bytes in size.

FIELD

[0003] The present invention generally relates to amplification methods useful for high-sensitivity assays.

BACKGROUND

[0004] Sequence-specific detection of low concentrations of nucleic acids, such as DNA and RNA, is typically achieved through the use of enzyme-catalyzed reactions, such as the polymerase chain reaction (PCR). In order to accommodate the enzyme catalysts these procedures require precise reaction conditions, detailed sample preparation, and carefully controlled reagent storage. Thus, these powerful tools are largely absent from all environments beyond centralized laboratories.

[0005] Sequence-specific nucleic acid detection is a key underpinning of genomics research in particular and biomedical research overall. This dominant technique, PCR, and all others available, including loop-mediated isothermal amplification (LAMP), self-sustained sequence replication (3SR), nucleic acid sequence-based amplification (NASBA), strand displacement amplification (SDA), and rolling circle amplification (RCA),

require enzymes to amplify the signal. The environmental sensitivities of the required enzymes has broadly limited these techniques to laboratory settings and added significant difficulties to their field use.

[0006] Nucleic acid amplification occurs in three general steps, which are performed sequentially across multiple cycles in order to amplify the signal, as is well known to those skilled in the art. First, the "template" strand of DNA to be amplified is denatured. Second, specific "primer" sequences, comprising strands of complementary oligonucleotides (oligos), bind at the 5' ends of the template strands. Third, a DNA polymerase enzyme elongates the entire template strand in the 5' to 3' direction, beginning where the primers have bound. Each cycle thus doubles the number of DNA strands, resulting in a 2^n amplification of the nucleic acid for n cycles.

SUMMARY OF INVENTION

[0007] Herein is described an enzyme-free technique for sequence-specific detection of nucleic acids with limits of detection similar to PCR. The technique is robust and well-suited for use in field environments because of its reliance on stable, small molecules for amplification, its use of standard optical components for detection, and its inherent multiplexibility.

[0008] Furthermore, enzyme-free amplification greatly eases restrictions on sample preparation as well as on the design of the oligonucleotide primers crucial for specificity. This approach is also suitable for high-sensitivity protein assays permitting, for the first time, a single platform to simultaneously perform high-sensitivity proteomic and genomic testing. This technology thus holds the promise to revolutionize high-sensitivity testing.

[0009] In particular, although powerful, enzyme-based techniques suffer from some or all of certain major drawbacks identified as follows. First, enzymatic activity can be greatly affected by sample purity. Thus, rigorous and precise sample preparations are required to ensure reproducible amplifications. Second, enzymes require careful storage and handling, generally preventing their use in field settings. Third, primer design is often

difficult, requiring the proper balance to be struck between competing requirements. This slows the adaptability of the technique to new sequences and often requires compromises in primer design, decreasing efficacy, specifically in the case of real time-PCR. Fourth, one or more additional steps, often requiring distinct enzymes, are needed for RNA detection. Fifth, the cycling and, specifically, thermal cycling requirement pose significant engineering hurdles for building small, easy-to-use devices required for field use. Sixth, this amplification process is sufficiently different from that underlying proteomics detection that different instruments and, often, multiple samples are necessary when proteomics and genomics information must both be known.

[0010] Multiple techniques have been suggested to decrease the number of PCR or similar cycles required to achieve high-sensitivity and sequence-specific nucleic acid detection. However, these all still require enzymatic amplification and, in turn, do not solve many of the core PCR issues.

[0011] Similarly, sensitive and specific protein and small molecule detection often requires enzyme-amplified immunoassays (EIAs), as known to those skilled in the art. Though of a different class, these enzymes suffer from similar limitations to those of PCR. It should be noted that in the specific case of the immune-PCR and bio-barcode techniques, the PCR enzymes are used to amplify protein signals. By relying on PCR amplification, these techniques significantly enhance the sensitivities of standard EIAs. However, their complexities and environmental sensitivities have limited their field use to date. Thus, there is a specific need for protein assays that offer greater sensitivities compared with current EIAs, as well.

[0012] Herein are disclosed novel techniques for enzyme-free highly sensitive and sequence-specific detection of nucleic acids, proteins, and small molecules. Similarly to PCR and related methods and immunoassays, specificity is achieved through the use of at least two primer sequences or antibodies that hybridize with the template nucleic acid or protein. Amplification is then performed in only two steps, though additional steps may be utilized.

[0013] In one aspect, the invention features a method of detecting one or more analytes in a sample comprising:

incubating a sample with a plurality of nanoparticles comprising one or more payloads comprising one or more recruiting agents, wherein each nanoparticle is functionalized with moieties enabling specific binding of an analyte and a plurality of capture particles is functionalized with moieties capable of binding the same analyte;

releasing the one or more recruiting agents from the nanoparticles bound to the analytes;

introducing a plurality of catalyst-comprising particles, each comprising one or more functionalities capable of specifically binding to the recruiting agent;

dissociating the catalyst-comprising particles bound to the recruiting agents thereby generating signals; and

determining the presence or quantity of the analyte in the sample based on the generated signals.

[0014] In another aspect, the invention features a kit for detecting one or more analytes in a sample comprising:

a plurality of nanoparticles comprising one or more payloads comprising one or more recruiting agents, wherein each nanoparticle is functionalized with moieties enabling specific binding of an analyte;

a plurality of capture particles functionalized with moieties capable of binding the same analyte;

a solution for releasing the one or more recruiting agents from the nanoparticles; and

a plurality of catalyst-comprising particles, each comprising one or more functionalities capable of specifically binding to the recruiting agent; and

a solution comprising reagents for performing a reaction that generates signals, once the catalyst is released.

BRIEF DESCRIPTION OF DRAWINGS

[0015] FIG. 1 is a schematic showing the steps in the cascaded-amplification processes used in detecting a specific nucleic acid sequence.

[0016] FIG. 2 is a primer design for nucleic acids and comparison with PCR primers.

[0017] FIG. 3 shows the TCO-Bz-Biot heterobifunctional crosslinker structure.

[0018] FIG. 4 shows FAMP particles comprising the TCO-Bz-Biot crosslinker in a poly(*L*-lactic acid) (500 kD) matrix.

[0019] FIG. 5 shows the release of the TCO-Bz-Biot crosslinker.

[0020] FIG. 6 shows a comparison of activities of horseradish peroxidase (HRP) enzyme (Sigma Aldrich) and small molecule catalyst, metal-tetraamidomacrocyclic ligand complex (MTALC or TAML; GreenOx Catalysts; US 6,100,394).

[0021] FIG. 7 shows effective containment of MTALC in SAMP particles.

[0022] FIG. 8 shows specific detection of *Listeria Monocytogenes* genomic DNA (obtained from ATCC, Inc.) was achieved with the cascaded-amplification process using primers specific for 16S rDNA genes.

[0023] FIG. 9 shows specific detection of Dengue synthetic RNA (obtained from ATCC, Inc.) was achieved with the cascaded-amplification process using primers given by ATCC.

[0024] FIG. 10 shows specific detection of *Yersinia Pestis* genomic DNA (obtained from ATCC, Inc) was achieved.

[0025] FIG. 11 shows specific detection of *Listeria Monocytogenes* bacteria was performed in spiked lettuce samples.

[0026] FIGS. 12A-12C shows a schematic of magnetic fractionation device (1201) (**FIG.12A**) and fluorescence micrographs of red channel-active magnetic particles 2.85 μm in diameter (1202) (**FIG.12B**) and green channel-active particles 0.86 μm in diameter (1203) (**FIG.12C**).

[0027] FIG. 13 shows a multiplexed *Y. Pestis* and Dengue test was performed at the highest dilution.

[0028] FIG. 14 shows a comparison of human chorionic gonadotropin (hCG) detection with standard ELISA ("HRP") and with FAMP particle binding and recruiting agent release followed by HRP signal generation ("FAMP").

[0029] FIGS. 15A-15E relate to CAN design and performance. **FIG. 15A** is a schematic illustration of nanolabels highlighting the key elements. **FIG. 15B**is a schematic illustration of (i) CAN binding in a sandwich immunoassay, (ii) subsequent CAN bursting to release the biotin-TCO crosslinker that binds surface Tz groups, and (iii) final binding of streptavidin-HRP for signal development. **FIG. 15C is a** CAN-amplification comparison with standard, HRP-based ELISA for *β*-hCG. Error bars represent ±1 standard deviation. **FIG. 15D is a** CAN-amplification comparison with tyramide amplified "high-sensitivity" ELISA for IL-6. Error bars represent ±1 standard deviation. **FIG. 15E** is a comparison of tyramide amplified ELISA and CAN amplification for 4 human plasma samples (HS) and 2 IVF embryo culture media samples. These were from a sample that comprised an embryo for 5 days (IVF 1) and a control sample without an embryo (IVF 2). The tyramide amplification datapoint for sample IVF 2 was below the detection threshold. Error bars represent ±1 standard deviation. For **FIGS. 15C-15E**, error bars may not be visible due to resolution constraints when the relative error is <5%. Experiments were repeated at least 3 times in triplicate with similar results.

[0030] FIGS. 16A-16E relate to SAL design, synthesis and performance. **FIG. 16A** is a schematic illustration of (i) SAL binding in a sandwich immunoassay and (ii) subsequent SAL bursting to release TAML for homogeneous catalysis. **FIG. 16B** is a catalytic comparison of HRP and TAML after 15-minute endpoint measurements. The plot compares results from optimal conditions for each catalyst and the inset shows the TAML chemical structure. The dashed lines are linear best fits for each dataset with R^2 of 0.997 for HRP and 0.987 for TAML. The signal was normalized to "1" at zero concentration. Errors were propagated and error bars represent ±1 standard deviation. **FIG. 16C** shows that during the oil-in-oil emulsion step, the dispersed phase (gray) comprises poly-*L*-lactic acid (PLLA) and TAML and is stabilized by a surfactant

(blue/black), poly(maleic anhydride-*alt*-octadecene). **FIG. 16D** shows that upon inversion into water, a crosslinked polystyrene shell (blue) comprising styrene and divinyl benzene is polymerized around the nanoparticle cores. These dispersed-phase reactions are stabilized by DSPE-PEG surfactants (green). **FIG. 16E** is a SAL-alone comparison with HRP-based ELISA for *C. difficile* Toxin A. The signal was normalized to "1" at zero concentration. Errors were propagated and error bars represent ±1 standard deviation. Error bars in **FIGS. 16B** and **16E** may not be visible due to resolution constraints when the relative error is <5%. Experiments were repeated 3 times in triplicate with similar results.

[0031] FIGS. 17A-17D relate to CAN-SAL cascade design and performance. **FIG. 17A** shows a schematic illustration of CAN-SAL cascade. i-iv depict the reaction scheme, as described in the text. The crosslinker structure is in **FIG. 3**. (**B**) Theoretical amplification abilities of assays based on an ELISA baseline of "1," as described in the text. The amplification of PCR relative to ELISA is based on the 1 pM HRP LoD determined in **FIG. 2B**, which corresponds to 6×10^7 molecules. (**C**) CAN-SAL detection of *L. monocytogenes* bacteria using a single CAN oligo sequence. Signals were normalized to "1" at zero DNA concentration and errors were propagated. Error bars represent ±1 standard deviation. (**D**) CAN-SAL detection of *L. monocytogenes* bacteria using four CAN oligo sequences permitting multiple CAN binding events per template strand. Signals were normalized to "1" at zero DNA concentration and errors were propagated. Error bars represent ±1 standard deviation. Error bars in panels (**C**) and (**D**) may not be visible due to resolution constraints when the relative error is <5%. Experiments were repeated 5 times in triplicate with similar results. *L. monocytogenes* isolates were selected on 3 different days.

[0032] FIGS. 18A-18C relate to CAN-SAL performance with low-cost SiPM detector. **FIG. 18A** shows CAN-SAL detection of purified *L. monocytogenes* DNA from buffer and complex media. Arrows show the "Low" (green) and "High" (blue) concentrations used in **FIG. 18C**. Signals were normalized to "1" at zero DNA concentration and errors were propagated. Error bars represent ±1 standard deviation. **FIG. 18B** shows a comparison of fluorescein detection with a PMT (Molecular Devices Spectramax M2) and a SiPM (inset). Signals were normalized to "1" at zero fluorescein concentration. **FIG. 18C** shows

a real-time SiPM fluorescence signal from microfluidic chip assays for the "Low" and "High" *L. monocytogenes* DNA dilutions from **FIG. 18A** and a *L. monocytogenes* DNA-free control sample. Datapoints were collected at a rate of 1 per second and each plotted series represents a single experiment. All experiments were repeated at least four times with similar results.

[0033] FIGS. 19A-19F relate to multiplex detection of DNA, RNA and proteins. **FIG.19A** is a schematic showing larger, red particles exhibiting increased magnetic susceptibility and exiting in the upper channel. Smaller, green particles remain in the lower channel. **FIGS. 19B** and **19C** are representative fluorescence optical micrographs of particles schematically illustrated in **FIG. 19A**. Larger, red fluorescent beads cross to the upper exit port (**FIG. 19B**), whereas the smaller, green fluorescent beads continue in the original stream (**FIG. 19C**). Note the red particles bleed into the green fluorescence channel. All experiments were repeated 3 times with similar results. **FIG. 19D** is a comparison of dengue RNA and *Y. pestis* DNA detection "alone" (for dengue RNA or *Y. Pestis* DNA alone) or by "multiplex" (assaying for both simultaneously in the same sample). Signals were normalized to "1" at zero DNA/RNA concentration and errors were propagated. Error bars represent ±1 standard deviation. Experiments were repeated 3 times with similar results. **FIG. 19E** is a comparison of PCR and CAN-SAL assays for *S. aureus* and MRSA from human BAL samples. Positive samples are defined as those with normalized signals ≥1.3 (see **FIG. 25B**). **FIG.19F** is a normalized α-Hla results for the same BAL samples. The hashed bar shows the α-Hla-positive *S. aureus* sample. All signals were normalized to "1" for zero-concentration α-Hla controls and errors were propagated. Error bars represent ±1 standard deviation. Experiments were repeated 3 times in triplicate with similar results.

[0034] FIG. 20 shows DLS and NanoSight analyses of SALs. These data show DLS as taken by a Malvern ZetaSizer and a laser optical image taken by a Malvern NanoSight of a representative SAL formulation. The PDI as determined by the ZetaSizer was 0.14.

[0035] FIG. 21 relates to storage stability of SALs. Comparison of newly synthesized and room temperature-stored USAs for performing a human cardiac troponin (cTnI) sandwich immunoassay. These data demonstrate the stability of the SAL platform.

Human cTnI antibodies and a commercial kit were purchased from RayBiotech. An assay similar to that for *C. difficile* Toxin A described in the Methods section was used.

[0036] FIG. 22 relates to thermal stability of CANs. The CAN-SAL cascade is further designed to give dual-primer/antibody specificity similar to that of PCR or ELISAs. Oligo-functionalized CANs bind to oligo-functionalized magnetic capture beads only if the proper template strand is present, **FIG. 15b(i)**. The oligo sequence comprised a complementary DNA sequence followed by two spacers equivalent to 4-5 basepairs in length, which have been shown to be sufficient spacing from nanoparticles for rapid binding[18]. CANs are designed for stability through 50°C, **FIG. 22**, and all CAN-template-magbead hybridizations are run at this temperature using standard PCR primers[7]. **FIG. 22** shows a measurement of the realease of TCO crosslinker from CANs after thermal treatments at different temperatures. Measurements were performed by coating a Nunc Maxisorp plate with Tz-BSA and using streptavidin-HRP (ThermoFisher) as the reporter. A standard curve was prepared using known concentrations of biotin-TCO crosslinker. Experiments were repeated 4 times with similar results.

[0037] FIG. 23 shows a primer design comparison between PCR and CAN-SAL assays. Multiple CAN oligos can bind a single DNA/RNA strand, in comparison with PCR primers, where only one may bind each strand. It is important that the sense of CAN "Primer 1" is reverse and complementary that of PCR "Primer 1."

[0038] FIGS. 24A-24B show microfluidic chip layouts. **FIG.24A** is an exploded view and **FIG. 24B** is a complete view of a microfluidic chip used for *L. monocytogenes* DNA detection. Up to three assays can be run on a same chip. Recesses in the top layer are for N52-grade niobium magnets and optical windows allow detection of optical signals.

[0039] FIGS. 25A-25B show CAN-SAL *S. aureus* and MRSA identification. **FIG.25A** is a comparison of PCR and CAN-SAL results for *S. aureus* (rRNA or rDNA) and MRSA (*mecA*) on 10 "blinded" samples. **FIG.25B** shows raw data from CAN-SAL assay for *S. aureus* rRNA and *mecA* shown in **FIG. 19E**.

DEFINITIONS

[0040] As used herein, the term "analyte" broadly refers to any substance to be analyzed, detected, measured, or quantified. Examples of analytes include, but are not limited to, nucleic acids (e.g., DNA, RNA, PNA, LNA, BNA, and/or combinations thereof), proteins, small molecules, organisms such as microorganisms, viruses, peptides, hormones, haptens, antigens, antibodies, receptors, enzymes, polysaccharides, chemicals, polymers, pathogens, toxins, organic drugs, inorganic drugs, cells, tissues, bacteria, fungi, algae, parasites, allergens, pollutants, and combinations thereof.

[0041] As used herein, the term "about" in relation to a numerical value *x* means, for example, $x \pm 10\%$.

[0042] As used herein, a "catalyst" (e.g., a transition-metal catalyst) is a substance that increases the rate of a chemical reaction without itself undergoing any permanent chemical change, so as to covert a suitable substrate to a product, wherein the conversion results in a signal change. In some instances, the conversion leads to presence of increase of a detectable signal, e.g., the product releases a signal while the substrate does not. In other cases, the conversion leads to the diminishing or reduction of a signal, e.g., the substrate releases a signal while the product does not. In embodiments, transition-metal catalysts described herein are precursors to the catalytically active species in a reaction.

DETAILED DESCRIPTION OF INVENTION

[0043] The simplicity, consistency, and competitive cost of enzyme-linked immunosorbent assays (ELISAs) for protein quantification and the polymerase chain reaction (PCR) for DNA and RNA detection account for their durability as dominant technologies. In comparison, next-generation sensing approaches offer significant potential for enhanced sensitivity and flexibility. However, many new molecular sensing platforms require expensive detection equipment, limiting widespread utility.

[0044] Herein is introduced a nanoparticle synthetic amplifier label ("SAL") that permits existing microplate readers to quantify proteins with >100-fold sensitivity versus ELISAs.

By developing a low-cost, robust fluorimeter, rapid platform translation from bench to a bedside point-of-care (POC) device can be achieved. The platform's ability to perform immunoassays as well as DNA and RNA assays – with sensitivities approaching quantitative PCR – by simultaneously identifying *Staphylococcus aureus* genetically and a specific protein toxin, α-hemolysin, by immunoassay is demonstrated. The SAL platform thus represents a novel, ultra-sensitive multiplex detection system that is compatible with current detector technology, potentially permitting rapid integration into high-volume laboratory testing in clinical and research settings.

[0045] Both ELISA and PCR technologies permit high-sensitivity protein and DNA/RNA detection from low-cost platforms (References 1-5). As a result, these technologies, along with electrochemiluminescent immunoassays (Reference 6), remain as dominant detection methodologies, despite the development of novel sensing platforms that offer significantly improved sensitivities beyond ELISAs and flexibilities beyond PCR (References 6-15). However, many of these alternative approaches require integration with optical, electrical, electrochemical, and/or nuclear magnetic resonance detection platforms (References 6-15). The cost associated with these systems has limited their utility for hospital laboratories as well as for research groups, and has prevented these technologies from widespread adoption. In contrast, optical platereaders are so useful for detecting outputs from ELISAs and PCR assays that they have become ubiquitous in laboratories at all levels. Thus, the ability to integrate novel, ultrasensitive sensing approaches with optical platereader detection may allow for a significant advance in molecular sensing that could be translated to large-scale use.

[0046] Among a variety of high-sensitivity assay technologies, nanoparticle labels ("nanolabels") have emerged as powerful *in vitro* assay amplifiers compatible with a myriad of detection platforms – including optical platereaders – offering enhanced sensitivities, dynamic ranges, and multiplexing capabilities (References 7-9,13-17). Nanolabels have been used effectively as bio-barcodes (References 7-9) and with electrochemical (13-15), nuclear magnetic resonance (Reference 16), and time-resolved fluorescence (Reference 17) detection platforms, among other approaches. Many of these approaches have been shown to extend limits of detection (LoDs) beyond the capabilities of natural enzymes. However, nanolabels designed for compatibility with

optical detection platforms have, to date, offered little to no improvement over standard ELISA sensitivities (References 18,19). This is, in part, due to diffusion limitations of heterogeneous catalysis (Reference 20). Early work demonstrated the potential of encapsulating a redox-active species within a nanolabel and then releasing it after a biochemical binding event to permit ultra-sensitive electrochemical detection (Reference 21). Yet, when this encapsulation-release approach has been translated to fluorescent molecules or metal ions for compatibility with existing optical systems, LoDs were similar to ELISAs (References 22-25).

[0047] Herein are described strategies for overcoming the traditional trade-off between existing platforms and high sensitivity by adapting recent targeted drug delivery formulation methods (References 26,27) to encapsulate organometallic catalysts with near-enzymatic kinetics (References 19,28,29). Upon chemically-triggered release following specific nanolabel binding, these molecules homogeneously catalyze optical signal development, permitting standard optical platereaders to achieve >100x sensitivity improvements over standard ELISAs. Additionally, the potential of multiplexing protein and nucleic acid assays on the same platform directly from complex samples was explored. Further, compatibility of the nanolabel approach with a silicone photomultiplier for potential point-of-care (POC) utility was evaluated.

[0048] In one aspect, the invention features a method of detecting one or more analytes in a sample comprising:

incubating a sample with a plurality of nanoparticles comprising one or more payloads comprising one or more recruiting agents, wherein each nanoparticle is functionalized with moieties capable of specific binding of an analyte and a plurality of capture particles is functionalized with moieties capable of binding the same analyte;

releasing the one or more recruiting agents from the nanoparticles bound to the analytes;

introducing a plurality of catalyst-comprising particles, each comprising one or more functionalities capable of specifically binding to the recruiting agent;

dissociating the catalyst-comprising particles bound to the recruiting agents thereby generating signals; and

determining the presence or quantity of the analyte in the sample based on the generated signals.

[0049] In embodiments, an analyte to be detected is independently a nucleic acid, a protein, a small molecule, an organism, or a virus.

[0050] In embodiments, an analyte to be detected is independently a nucleic acid.

[0051] In embodiments, a nucleic acid is independently a DNA or RNA.

[0052] In embodiments, moieties on the recruiting agent-comprising nanoparticles and the capture particles bind one or more different regions of the analyte to be detected.

[0053] In embodiments, a recruiting agent-comprising nanoparticles and the capture particles each falls into the size range of 25 nm to 10 microns (e.g., 25 nm to 1 micron, 25 nm to 500 nm, 25 nm to 250 nm, or 25 nm to 100 nm).

[0054] In embodiments, a recruiting agent-comprising nanoparticles comprise an enzyme conjugate to facilitate signal generation.

[0055] In embodiments, an enzyme is HRP, AP, and/or ACE.

[0056] In embodiments, capture particles are susceptible to an external magnetic, optical, and/or acoustic field and/or a size exclusion gradient.

[0057] In embodiments, recruiting agents are chemical and/or biochemical crosslinkers, comprising one or more of the same or different functional moieties.

[0058] In embodiments, a catalyst-comprising species is one or more of particulate, enzymatic, and/or polymeric in nature.

[0059] In embodiments, a generated signal is optical and/or electronic.

[0060] In embodiments, particles bound to the analytes are addressable.

[0061] In embodiments, addressable particles are susceptible to different fields and/or gradients such that multiple analytes are detected in parallel.

[0062] In embodiments, a method further comprises mixing steps to prevent settling of the particles.

[0063] In embodiments, a method is performed in a glass, polymeric, or metallic vessel and/or microfluidic platform.

[0064] In embodiments, moieties on the recruiting agent are bound to a solid support.

[0065] In embodiments, a solid support is a particle susceptible to an external magnetic, optical, and/or acoustic field and/or a size exclusion gradient.

[0066] In embodiments, a sample pre-treatment is performed prior to the onset of the assay.

[0067] In embodiments, one or more of the moieties specific for the analytes to be detected is not functionalized to the recruiting agent-comprising nanoparticles and/or capture particles at the time of binding but, rather, binds one or more of these particle types after binding the analyte to be detected.

[0068] In embodiments, a recruiting agent reacts with the catalyst-comprising particles to expose the catalyst.

[0069] In embodiments, a method comprises adding one or more additional recruiting agent-comprising nanoparticles for multi-tiered amplification.

[0070] In embodiments, a recruiting agent-comprising nanoparticles or the catalyst-comprising particles do not comprise protein signal precursor molecules and/or carrier protein.

[0071] In another aspect, the invention features a kit for detecting one or more analytes in a sample comprising:

a plurality of nanoparticles comprising one or more payloads comprising one or more recruiting agents, wherein each nanoparticle is functionalized with moieties enabling specific binding of an analyte;

a plurality of capture particles functionalized with moieties capable of binding the same analyte;

a solution for releasing the one or more recruiting agents from the nanoparticles; and

a plurality of catalyst-comprising particles, each comprising one or more functionalities capable of specifically binding to the recruiting agent; and

a solution comprising reagents for performing a reaction that generates signals, once the catalyst is released.

[0072] In embodiments, a recruiting agent-comprising nanoparticles and the capture particles each fall into the size range of 25 nm to 10 microns (e.g., 25 nm to 1 micron, 25 nm to 500 nm, 25 nm to 250 nm, or 25 nm to 100 nm).

[0073] In embodiments, a recruiting agent-comprising nanoparticles comprise an enzyme conjugate to facilitate signal generation.

[0074] In embodiments, an enzyme is HRP, AP, and/or ACE.

[0075] In embodiments, recruiting agents are chemical and/or biochemical crosslinkers, comprising one or more of the same or different functional moieties.

[0076] In embodiments, a catalyst-comprising species is one or more of particulate, enzymatic, and/or polymeric in nature.

[0077] In embodiments, a kit further comprises a glass, polymeric, or metallic vessel and/or microfluidic platform.

[0078] In embodiments, a kit further comprises a solid support.

[0079] In embodiments, a recruiting agent-comprising nanoparticles or the catalyst-comprising particles do not comprise protein signal precursor molecules and/or carrier protein.

Exemplary Methods

[0080] Exemplary embodiments are described as follows.

[0081] FIG. 1 is a schematic showing the steps in the cascaded-amplification processes used in detecting a specific nucleic acid sequence. Capture particles (101), FAMP particles (102), and SAMP particles (103), are all shown. The recruiting agent payload (104) and MTALC (also referred to as TAML) catalyst (105) are also illustrated. Note in this schematic the solid surface binding partner of the recruiting agent is present on the capture particles themselves.

[0082] FIG. 2 is a primer design for nucleic acids and comparison with PCR primers. Standard PCR primers are shown as 201 and 202. These are each designed to bind the 3' end of different strands of the template region. Cascaded amplification requires binding to each template strand at least one capture particle and at least one FAMP particle. (Both strands may be used.) Thus primer 203, which binds the capture particle, and 204 and 205, which bind the FAMP particle, all bind a single template strand.

[0083] FIG. 3 shows the TCO-Bz-Biot heterobifunctional crosslinker structure. The *trans*-cyclooctene was selected because of its rapid reaction kinetics with tetrazine and the irreversibility of the resulting bond (Patterson *et al. ACS Chem. Biol.* Vol. 9 (2014), 592). The biotin was selected because of its rapid binding kinetics with avidin (including streptavidin and neutravidin) and the very low dissociation constant of the existing bond (Patterson *et al. ACS Chem. Biol.* Vol. 9 (2014), 592). The benzene-comprising linker between the functional endgroups was chosen for its low aqueous solubility.

[0084] Preceding the first amplification step, two particles functionalized with different oligomer primers or antibodies bind the template nucleic acid or protein. In contrast to PCR primers, which bind complementary strands of the same template region, the primers described herein are designed to both bind the same template strand. The "capture" particle is magnetically addressable and the first-amplification "FAMP" particle comprises a "recruiting agent" payload, such as a chemical crosslinker. This crosslinker is sealed within the FAMP particles, which are designed to be stable in neutral aqueous solutions. In order to replicate the specificity of PCR, the particles are designed to permit primer hybridization at 50-55°C. Since template denaturing occurs at temperatures greater than 90°C, the particle solution is added immediately upon sample cooling to 50-55°C.

[0085] In embodiments, a first-amplification "FAMP" particle is a recruiting agent-comprising nanoparticle as described herein.

[0086] Following hybridization or antibody binding, capture particles are trapped in a magnetic field and thoroughly washed. If present, template strands tether FAMP particles to the capture particles; thus FAMP particles remain after washing only when template strands are present. For cases where very low numbers of template strands must be detected, FAMP particles with multiple oligomer sequences specific for different regions of each template strand may be used such that multiple FAMP particles bind each template strand. Furthermore, this design may be replicated on both complementary strands. In contrast to enzyme-based amplification methods, such as PCR, this technique permits direct RNA detection, thus there is no need for RNA-to-DNA conversion.

[0087] The first amplification step occurs when bound FAMP particles are "burst" to release the chemical crosslinker. This may be achieved with one or more of: a change in pH, a non-water solvent, and/or a physical trigger such as light, heat, or sonic energy.

[0088] The released crosslinker, an example of which is the heterobifunctional crosslinker biotin-benzyl-trans-cycloolefin, may then bind to a reactive moiety on a solid support, such as tetrazine. This support may be the surface of the chamber or channel or the surface of a particle and/or bead, including the capture particles themselves. In the case of a heterobifunctional crosslinker, the solid support may be functionalized with a chemical moiety capable of reacting with one of the crosslinker's groups. Thus, upon release the crosslinker effectively becomes surface-bound. In the case where electrochemical detection is performed, the functionalized solid support may be in the vicinity of the electrode.

[0089] The crosslinker may be designed for minimal aqueous solubility in the pH range of primer and/or protein binding. Soluble binding partners for the crosslinker may be included in the solution during primer binding to "catch" any crosslinkers released at this stage. In some embodiments, aqueous-soluble crosslinkers may be advantageous.

Crosslinker solubility may be tuned by altering the linking groups, which can include benzene, phenyl, or similar aromatics, ethylene oxide groups, or aliphatic groups.

[0090] Each FAMP particle may comprise 10^2-10^7 crosslinkers, and more preferably 10^3-10^6. The ideal first amplification factor is defined as the number of crosslinkers per FAMP particle times the number of bound FAMP particles. The real amplification factor may be lower than ideal due to incomplete crosslinker binding, crosslinker loss, or other effects.

[0091] Following binding of the crosslinker to the surface, second-amplification "SAMP" particles are introduced that bind the free functional moiety of the crosslinker, such as with neutravidin. These SAMP particles comprise a signal generating payload, such as a catalyst, as described in US Application Numbers 62/029,270; 62/142,721; 62/053,250; 62/194,038; 62/194,046; 62/194,062; 14/809,116; and PCT/US2015/042133**,** which are incorporated fully by reference herein. After thorough washing to remove unbound SAMP particles, these particles are "burst" to release the catalyst, which catalyzes a signal-generating reaction, such as a reaction that produces an optical and/or electrochemical signal.

[0092] In embodiments, a second-amplification "SAMP" particle is a particle comprising a signal-generating agent (e.g., a catalyst-comprising particle) as described herein.

[0093] Each SAMP particle may comprise 10^2-10^7 signal generating agents, and more preferably 10^3-10^6. The ideal second amplification factor is thus the multiple of the number of catalysts per SAMP particle and the catalytic activity of the catalyst itself.

[0094] In a representative embodiment, there are $1x10^5$ heterobifunctional crosslinkers per FAMP particle and $1x10^4$ TAML catalysts per SAMP particle. These catalysts are fluorescently detectable at a concentration of $1x10^{-11}$ M at a volume of $3x10^{-4}$ L. Thus, the template strand is theoretically detectable down to 1.8 molecules, although this fails to account for non-specific binding.

Exemplary Kits and Components for Performing the Methods

[0095] The present disclosure also provides kits for use in performing the methods described herein.

[0096] Such kits can comprise one, two, three, four, or five of the following components:

(1) a plurality of FAMP particles (e.g., nanoparticles comprising one or more payloads comprising one or more recruiting agents), wherein each FAMP (e.g., a nanoparticle) is independently functionalized with moieties enabling specific binding of an analyte;

(2) a plurality of capture particles independently functionalized with moieties capable of binding the same analyte;

(3) a solution for releasing the one or more recruiting agents from the nanoparticles;

(4) a plurality of SAMP particles (e.g., catalyst-comprising particles), each comprising one or more functionalities capable of specifically binding to the recruiting agent; and

(5) a solution comprising reagents for performing a reaction that generates signals, once the catalyst is released.

[0097] A kit may further comprise other components for performing the method. For example, a kit may further comprise a glass, polymeric, or metallic vessel and/or microfluidic platform. In embodiments, a kit further comprises a solid support.

Additional Embodiments

[0098] Still further embodiments are described herein.

[0099] Samples may be derived from any biological, chemical, and/or other source. The detection events may occur, e.g., in one or more of the following platforms: tubes, plates, automated, microfluidic.

[0100] Capture particles addressable by any external force may be used. Examples include, but are not limited to, particles with magnetic susceptibility; particles separable by size

exclusion; particles addressable by optical, acoustic, or electrical trapping and/or gradients; and particles with specific surface functionalities to permit separation.

[0101] In certain embodiments, surfaces used for capture may also be macroscale, such as microplate wells. Macroscale surfaces may also be used for binding of a recruiting agent. These may be the same and/or different surfaces from those used for capture.

[0102] In embodiments, capture particles independently each fall into the size range of about 25 nm to about 10 microns (e.g., about 25 nm to about 1 micron, about 25 nm to about 500 nm, about 25 nm to about 250 nm, or about 25 nm to about 100 nm).

[0103] In embodiments, capture particles are susceptible to an external magnetic, optical, and/or acoustic field, and/or a size exclusion gradient.

[0104] In embodiments, capture particles are magnetically addressable (e.g., susceptible to an external magnetic field).

[0105] In embodiments, two different recruiting agents may be required in order for SAMP particles to bind. In this case, two different FAMP particles with different oligo-functionalized surfaces would be required in order for a SAMP particle to bind.

[0106] In other embodiments capture particles requiring fields of different strength may be used for differential capture. By using two different sized magnetic particles, split flow microfluidic cells, may be used to multiplex samples.

[0107] A primer may be of any nucleic acid type known to those skilled in the art comprising, but not limited to, DNA, RNA, PNA, LNA, BNA, and/or combinations. Primers may or may not be fully complementary. Primers may further comprise other molecules with binding partners including, but not limited to, e.g. aptamers, antibodies, receptors, ligands, cofactors, antagonists, glycoproteins, sugars.

[0108] Template strand(s) may similarly be one or more of any nucleic acid type or multiple types including, but not limited to, DNA, RNA, PNA, LNA, BNA, and/or combinations thereof. The definition of template strands may be further expanded to comprise any molecule and/or species with one or more binding partners including, but not limited to,

e.g. aptamers, antibodies, receptors, ligands, cofactors, antagonists, glycoproteins, sugars, viruses, bacteria, fungi, yeast.

[0109] In embodiments, one or more primers may not be bound to capture and/or FAMP particles but may comprise one or more moieties capable of binding to species functionalized on the surface of capture and/or FAMP particles. These moieties may include, but are not limited to, e.g. one or more nucleic acid sequences, antibodies, receptors, other proteins, ligands, cofactors, antagonists, glycoproteins, sugars, reactive groups including thiols, amines, hydrazides, carboxylic acids, aldehydes, ketones, maleimides, tetrazines, alkynes, strained alkynes, azides, trans-cyclooctene.

[0110] Multiple capture and/or FAMP particles may be employed to detect a single template region. Capture particles may bind each template strand or may bind multiple strands resulting from a restriction digest, as known to those skilled in the art. FAMP particles may bind at multiple sites along a template strand.

[0111] FAMP particles may range in diameter that is about 25 to about 5000 nm. These particles may comprise one or more recruiting agent payloads, one or more matrix-forming agents, and one or more species for specific surface functionalization with primers.

[0112] In embodiments, a FAMP particle is a recruiting agent-comprising nanoparticle.

[0113] The matrix forming agent(s) may be designed to maintain integrity at moderate temperatures, 50-60°C, and to release the crosslinker upon introduction of a specific stimulus to provide, e.g., a dissociable FAMP particle (e.g., a dissociable recruiting agent-comprising nanoparticle). Exemplary dissociable matrices (matrices that can dissociate upon introduction of a specific stimulus or trigger) are described in US Application Numbers 62/029,270; 62/142,721; 62/053,250; 62/194,038; 62/194,046; 62/194,062; and 14/809,116; as well as International Application Nos. PCT/US2015/042133 and PCT/US2016/042589, each of which is incorporated by reference in its entirety: this may be a chemical reaction and/or solvation event or a physical stimulus.

[0114] In embodiments, FAMP particles (e.g., recruiting agent-comprising nanoparticles) are independently dissociable (e.g., a FAMP particle can be dissociated under, e.g., a physical trigger or a chemical trigger to release, e.g., a crosslinker). A suitable trigger for dissociating a particular FAMP particle (e.g., a recruiting agent-comprising nanoparticle) would depend on the materials used for making said recruiting agent-comprising nanoparticle, which is within the knowledge of a skilled person in the art. Exemplary triggers are described in, e.g., Table 2 of International Application No. PCT/US2016/042589, which is hereby incorporated by reference in its entirety, and include: a change in pH, a non-water solvent, and/or a physical trigger such as light, heat, or sonic energy.

[0115] In embodiments, a suitable trigger for dissociation of a particular FAMP particle (e.g., a recruiting agent-comprising nanoparticle) is different from a suitable trigger for dissociation of a particular SAMP particle (e.g., a catalyst-comprising species) included in the same kit and/or for use in the same method.

[0116] In embodiments, FAMP particles (e.g., recruiting agent-comprising nanoparticles) independently each fall into the size range of about 25 nm to about 10 microns (e.g., about 25 nm to about 1 micron, about 25 nm to about 500 nm, about 25 nm to about 250 nm, or about 25 nm to about 100 nm).

[0117] In embodiments, FAMP particles (e.g., recruiting agent-comprising nanoparticles) comprise an enzyme conjugate to facilitate signal generation. In embodiments, an enzyme is HRP, AP, and/or ACE.

[0118] In embodiments, a FAMP particle (e.g., a recruiting agent-comprising nanoparticle) independently comprises an oligomer primer or an antibody for binding a target (e.g., a nucleic acid or protein, respectively). In embodiments, said oligomer primer or said antibody binds the same target as a capture particle included in the same kit or to be used in the same method.

[0119] In embodiments, FAMP particles (e.g., recruiting agent-comprising nanoparticles) independently comprise different oligomer sequences specific for different regions of a template strand.

[0120] In embodiments, a kit comprises two or more (e.g., two or more, three or more, four or more, five or more, six or more, etc.) FAMP particles (e.g., recruiting agent-comprising nanoparticles), each independently comprising a different oligomer sequences specific for a different region of a template strand.

[0121] In embodiments, a method comprises the use of two or more (e.g., two or more, three or more, four or more, five or more, six or more, etc.) FAMP particles (e.g., recruiting agent-comprising nanoparticles), each independently comprising a different oligomer sequences specific for a different region of a template strand.

[0122] A recruiting agent may be a crosslinker, such as a heterobifunctional crosslinker or homobifunctional crosslinker.

[0123] In embodiments, recruiting agents comprise chemical and/or biochemical crosslinkers, comprising one or more of the same or different functional moieties. In embodiments, a recruiting agent comprises a chemical crosslinker.

[0124] In embodiments, a crosslinker is a heterobifunctional crosslinker.

[0125] In embodiments, a crosslinker is water-soluble.

[0126] In embodiments, a crosslinker comprises a functional group that modulates water solubility (e.g., a crosslinker comprises: benzene, phenyl, or similar aromatics; ethylene oxide groups; or aliphatic groups).

[0127] A crosslinker may also have more than two reactive moieties. Crosslinkers comprising two or more of the same reactive moiety may be designed to be sufficiently small to ensure only one moiety can bind its surface-immobilized binding partner. Reactive moieties include, but are not limited to, *e.g.* one or more of the following: TCO, tetrazine, biotin, avidin, streptavidin, neutravidin, thiobiotin, alkyne, strained alkyne, azide, NHS ester, carboxyl, amine, thiol, maleimide, isocyanate, isothiocyanate.

[0128] In embodiments, a crosslinker comprises a functional moiety that comprises an amine, carboxylic acid, thiol, azide, alkene (e.g., cycloalkene or terminal alkene), alkyne

(e.g., cycloalkyne or terminal alkyne), Ni, histidine, Cu, lysine, maleimide, NHS-ester, biotin, or a biotin-binding protein (e.g., avidin or streptavidin), or a combination thereof.

[0129] In embodiments, a crosslinker is a biotin-benzyl-trans-cycloolefin (e.g., as described herein).

[0130] In embodiments, a cross-linker comprises a functional group that can bind to a reactive moiety on a solid support as described herein.

[0131] In embodiments, a recruiting agent-comprising nanoparticle independently comprises about 10^2 to about 10^7 crosslinkers (e.g., about 10^3 to about 10^6 crosslinkers).

[0132] In embodiments, recruiting agent-comprising nanoparticles do not comprise protein signal precursor molecules and/or carrier protein.

[0133] Recruiting agents may also release the amplifiers of the SAMP particles (e.g., catalyst-comprising particles) by acting to increase the porosity and/or decrease the integrity of these particles. Examples include, but are not limited to, metals that intercalate in the membranes of particles or that adjust the solubility of SAMP particles or constituents by releasing a pH modulating, reducing, oxidizing, or solvent.

[0134] In order to permit multiple samples to be detected in parallel (multiplex detection), different FAMP particles may comprise different recruiting agents. At least one functional moiety on each recruiting agent may be different in order to permit such multiplexing. Functional groups for this use may be expanded to include small molecules capable of specific antibody binding, such as steroids, cholesterol, etc.; nucleic acids; polymer nucleic acids; or similar species.

[0135] Released recruiting agents may bind to the same or different surfaces to which the FAMP particles bound. In embodiments, released recruiting agents may bind to the same template molecules to which the FAMP particles

[0136] In order to expand the detection range of assays, FAMP particles may be prepared to additionally include signaling agents, signaling agent precursors, and/or signal generating agents, as described in US Application Numbers 62/029,270; 62/142,721;

62/053,250; 62/194,038; 62/194,046; 62/194,062; and 14/809,116; as well as International Application Nos. PCT/US2015/042133 and PCT/US2016/042589. In embodiments, a signaling agent in a FAMP particle is a catalyst (e.g., TAML) as described herein.

[0137] The matrix-forming agents of the FAMP particles may be the recruiting agents themselves or may be polymeric, inorganic, waxy, surfactant, etc. These particles may be solid or micellar or water-filled, e.g. liposomal.

[0138] FAMP species further be comprised of a block-copolymer comprising a primer head-group and a tail-group comprising pendant functional moieties capable of reacting and/or binding to the exposed SAMP functional groups. This offers the advantage of obviating the need for the FAMP-bursting (FAMP dissociation) step but at the cost of decrease of the first amplification factor.

[0139] In embodiments, SAMP particles comprise a signal-generating payload (e.g., a catalyst).

[0140] In embodiments, a SAMP particle is a catalyst-comprising particle.

[0141] In embodiments, a SAMP particle is a catalyst-comprising nanoparticle.

[0142] In embodiments, a SAMP particle comprises a catalyst as described in any of US Application Numbers 62/029,270; 62/142,721; 62/053,250; 62/194,038; 62/194,046; 62/194,062; and 14/809,116; as well as International Application Nos. PCT/US2015/042133 and PCT/US2016/042589, which are incorporated fully by reference herein.

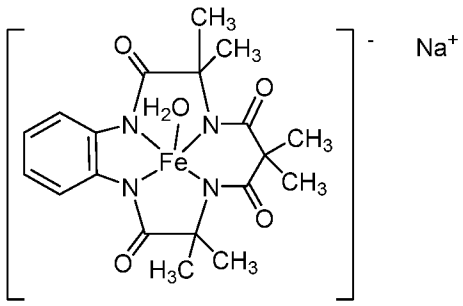
[0143] In embodiments, a catalyst is a metalorganic compound, which is a complex comprising a metal core (e.g., Fe, Mg, Cu, Mn, Pd, Pt, Ag, Ru, or Ce) and one or more organic ligands, e.g., porphyrin, substituted porphyrins, bipyridyls, bis-diimines, polydentates, ethanediamines, ethylenediamines, pentaaminecarbonatos, tetraaminecarbonatos, coumarins. Specific examples include, but are not limited to, iron porphyrins, hemin, ruthenium diimines, ruthenium bipyridyls, iridium-coumarin

complexes, bis(1,2-ethanediamine)copper, nickel porphyrin, and/or calcium ethylenediamine tetraacetate.

[0144] In embodiments, a catalyst that is a metalorganic compound comprises a metal core that is Fe.

[0145] In embodiments, a catalyst has a structure such as that described in any of U.S. Patent Nos. 6,100,394; 8,722,881; and 8,754,206, each of which is hereby incorporated by reference in its entirety.

[0146] In embodiments, a catalyst is, comprises, or is formed from Fe(III)-TAML® (sodium salt) metalorganic compound purchased from GreenOx (see, e.g., US Patent No. 6,100,394, which is incorporated herein by reference in its entirety) having the following structure,



("TAML").

[0147] In embodiments, a SAMP (e.g., a catalyst-comprising species) is particulate in nature, enzymatic in nature, and/or polymeric in nature. In embodiments, a SAMP (e.g., a catalyst-comprising species) is particulate. In embodiments, a SAMP (e.g., a catalyst-comprising species) is enzymatic. In embodiments, a SAMP (e.g., a catalyst-comprising species) is polymeric.

[0148] In embodiments, a SAMP (e.g., a catalyst-comprising species) does not comprise protein signal precursor molecules and/or carrier protein.

[0149] In embodiments, a SAMP (e.g., a catalyst-comprising species) is dissociable (e.g., a SAMP can be dissociated under, e.g., a physical trigger or a chemical trigger). A suitable trigger for dissociating a particular SAMP (e.g., a catalyst-comprising species) would

depend on the materials used for making said dissociable SAMP (e.g., a dissociable catalyst-comprising species), which is within the knowledge of a skilled person in the art.

[0150] A SAMP particle that is dissociable may comprise one or more matrix forming agents, which may be designed to maintain integrity at moderate temperatures (e.g., 50-60°C) and to effect dissociation upon introduction of a specific stimulus. Exemplary dissociable matrices are described in US Application Numbers 62/029,270; 62/142,721; 62/053,250; 62/194,038; 62/194,046; 62/194,062; and 14/809,116; as well as International Application Nos. PCT/US2015/042133 and PCT/US2016/042589, each of which is incorporated by reference in its entirety: this may be a chemical reaction and/or solvation event or a physical stimulus.

[0151] Exemplary triggers are described in, e.g., Table 2 of International Application No. PCT/US2016/042589, which is hereby incorporated by reference in its entirety, and include: a change in pH, a non-water solvent, and/or a physical trigger such as light, heat, or sonic energy.

[0152] In embodiments, a SAMP (e.g., a catalyst-comprising species) comprises about 10^2 to about 10^7 signal generating agents (e.g., about 10^3 to about 10^6).

[0153] In embodiments, a second amplification factor is the multiple of the number of catalysts per SAMP particle and the catalytic activity of the catalyst itself.

[0154] In embodiments, a SAMP (e.g., a catalyst-comprising species) comprises a moiety that binds a free (unbound) group on a crosslinker. For example, when a crosslinker comprises biotin, a catalyst-comprising species comprises a biotin-binding protein such as neutravidin. Similarly, when a crosslinker comprises a biotin-binding protein such as neutravidin, a catalyst-comprising species comprises biotin.

[0155] SAMP particles may be replaced with or used in parallel with one or more enzyme conjugates with reactive binding moieties, such as horseradish peroxidase-streptavidin, alkaline phosphatase-streptavidin, etc. They may also be replaced with a polymer chain with multiple signal generating groups in the backbone or pendant groups of the

polymer. The outlined steps of the process need not occur sequentially. The FAMP and SAMP particles may be designed such that multiple steps may be performed in parallel.

EXAMPLES

Example 1.

[0156] Capture particle conjugation. NHS-ester-functionalized superparamagnetic microparticles and nanoparticles were purchased from Bioclone and Ocean Nanotechnology, respectively. Oligonucleotides terminated with a 3' amino modifier were purchased from Integrated DNA Technologies (IDT). Starting at the 5' termini, these oligos comprised the primer sequence, followed by a "C18" spacer, and finally the 3' amino termination. Oligo-particle conjugation was performed according to the Bioclone instructions: particles at 200 mg/mL were suspended in a 5 μg/mL solution of the oligo in the Bioclone suspension buffer. The sample was vortexed to ensure particles were suspended and then reacted overnight at 50°C. After 12 hours, the beads were washed twice with the Bioclone wash buffer using a magnetic separation stand (Promega) and then twice with deionized water at 50°C. The particles were resuspended at a 20 mg/mL concentration in 1x SSC buffer and stored at 4°C until use. Optical density measurements of the oligo solution before and after reactions at 280 nm were used to confirm conjugation.

Example 2.

[0157] FAMP particles were synthesized with TCO-Bz-Biot (Conju-Probe) as the payload and poly(*L*-lactic acid) (PLA; 500 kDa; PolySciTech) as the matrix forming agent. In order to confer thiol reactivity to the particle surface, a poly(lactic acid)-poly(ethylene glycol)-maleimide block co-polymer of 30 kD:5 kD size was used (PolySciTech). These materials were dissolved in 2 mL chloroform in a 1:10:2 mass ratio. The resulting solution was then added to chloroform-saturated deionized water (0.815% chloroform in water) comprising 0.1% sodium dodecyl sulfate. The suspension was homogenized at 7,500 rpm (IKA) forming a milky, stable suspension. This was subsequently added to a >300 mL solution of water, which clarified the solution. Because of the maleimide instability in aqueous solutions, the pH of the water was titrated to ~5.0 with dilute hydrochloric acid.

[0158] After clarification the particle solution was immediately filtered through a 300 kD membrane (Millipore). The particles were concentrated to ~10 mL and measured with DLS. Particles were reacted with 5'-thiol-terminated oligonucleotides (IDT). The oligo sequence was 5'-dithiol endcap followed by a "C18" spacer, followed by the complementary DNA sequence. The thiol-maleimide reaction proceeded at room temperature for 2 hours in 1x PBS, pH 7.2 in the presence of 0.1 M tris(2-carboxyethyl)phosphine. Conjugation efficacy was determined with optical density absorbance readings at 280 nm with turbidity controls at 320 nm. Reacted particles were dialyzed into 1x SSC buffer and stored at 4°C.

[0159] **FIG. 4** shows FAMP particles comprising the TCO-Bz-Biot crosslinker in a poly(*L*-lactic acid) (500 kD) matrix were tested for their thermal stability. Dynamic light scattering (DLS) measurements were performed using a Malvern ZetaSizer. These show a monodisperse starting particle population ("start") with a mean diameter of 133 nm and a polydispersity index (PDI) of 0.128. DLS following 50°C treatment for 30 minutes show similar monodispersity ("50°C"), mean diameter (133 nm), and PDI (0.127). DLS following 55°C treatment for 30 minutes again show similar monodispersity ("55°C"), mean diameter (133 nm), and PDI (0.127).

Example 3.

[0160] FAMP release test. Bovine serum albumin (BSA) was functionalized with tetrazine using a NHS-reactive tetrazine crosslinker (Conju-Probe) and was bound to a MaxiSorp (Nunc) microplate in pH 9.5 sodium bicarbonate buffer. The filtrate was then introduced to the wells and the reaction was allowed to proceed for 1 hour at room temperature. A control dilution series "standard" was obtained using known concentrations of TCO-Bz-Biot in the same reaction buffer. After washing with 1x PBS comprising 0.02% Tween 20 (PBST), a streptavidin-horseradish peroxidase conjugate (ThermoFisher) was introduced and binding was allowed to proceed for 1 hour at room temperature. Washing with PBST was again performed followed by the addition of 3,3',5,5'-tetramethylbenzidine (TMB) solution comprising hydrogen peroxide (ThermoFisher). Following addition of a sulfuric acid stop solution, the absorbance was read at 650 nm.

[0161] FIG. 5 shows the release of the TCO-Bz-Biot crosslinker was determined for 30 minute incubations at 50°C and 55°C and compared with storage at room temperature. Experiments were conducted in 1x SSC buffer comprising 20 nM salmon sperm DNA and 0.001% Tween 20. Measurements are reported as the percent of initial encapsulated TCO-Bz-Biot in the particles, which was determined using a Malvern NanoSight analyzer. Released crosslinker was separated from FAMP particles after thermal treatment by filtering the solution through a 20 kD cutoff microfuge spin filter (VWR) and using the filtrate. Quantification was performed with a plate-based assay. The sample treated at 50°C showed negligible release compared with baseline. The sample treated at 55°C showed ~5% release. All samples were run in triplicate and error bars show standard deviation.

Example 4.

[0162] SAMP particles were formulated according to the methods described in US Provisional Application entitled "Water-inverted oil-oil nanoparticle formulation for hydrophilic species encapsulation", field on even date. Briefly, an inverted oil-in-oil emulsion technique was used. Poly(lactic acid)-diacrylate (20 kD; PolySciTech) and the MTALC iron salt (also referred to as "TAML;" GreenOx Catalysts) were dissolved in acetonitrile in a 5:1 mass ratio. A solution of poly(maleic anhydride-*alt*-octadecane) (PMAOD) in cyclohexanes was prepared and the acetonitrile solution was added and homogenized into the cyclohexanes at 7,500 rpm (IKA), forming a stable, milky emulsion. Benzene was then added to clarify the suspension. 1,2-distearoyl-sn-glycero-3-phosphoethanolamine-*N*-[biotinyl(polyethylene glycol)-2000] (DSPE-PEG-biotin; Laysan Bio) was then added in addition to 2,2'-azosisobutyronitrile (AIBN), styrene, and divinyl benzene. This solution was homogenized into a 5x volume of deionized water, forming a stable, milky emulsion with water as the continuous phase. The suspension was loaded into a round-bottom flask fitted with a reflux condenser, flushed with nitrogen, heated to 50°C and stirred at 400 rpm such that a vortex formed in the flask. The reaction proceeded for 2 hours, after which the heat was removed and the suspension was decanted into an open beaker, which was stirred overnight in a chemical fume hood to permit solvent evaporation. The resulting particles were filtered and

concentrated with a 300 kD membrane (EMD Merck) and measured by DLS and NanoSight techniques.

Example 5.

[0163] In order to determine the concentration of MTALC in the core of SAMP particles it was necessary to remove MTALC associated with but not bound within the particles. This was achieved with subsequent washes of the SAMP particles in a 300 kD-cutoff microfuge spin-filter column (VWR). Washes were performed with PBST and filtrates were collected. MTALC concentrations were determined fluorescent with the addition of 0.1 M sodium bicarbonate buffer (pH ~10) comprising 30 μM hydrogen peroxide and 600 μM DCFH-DA. Particles were resuspended in PBST for each wash by pipetting up-and-down five times. The final MTALC determination was made by first introducing acetone to the filter and pipetting up-and-down, followed by the addition of 0.1 M sodium bicarbonate buffer (pH ~10), followed by centrifugation and collection. Standard curves were established with soluble MTALC for quantification and particle loading was determined using a NanoSight to measure particle concentration. The resulting calculations show an MTALC loading of ~60,000 per nanoparticle.

[0164] FIG. 6 shows a comparison of activities of horseradish peroxidase (HRP) enzyme (Sigma Aldrich) and small molecule catalyst, metal-tetraamidomacrocyclic ligand complex (MTALC or TAML; GreenOx Catalysts; US 6,100,394). The molar activity of HRP is found to be ~10-fold greater than that of MTALC. The molecular weight of HRP is ~44,000 g/mol and the molecular weight of MTALC is ~650 g/mol, thus MTALC has a ~6.5-fold greater per-mass activity. HRP activity was measured using a commercial 3,3',5,5'-tetramethylbenzidine (TMB) solution comprising hydrogen peroxide at pH ~5.5 (ThermoFisher). MTALC activity was determined in a 0.1 M sodium bicarbonate buffer (pH ~10) comprising 30 μM hydrogen peroxide and 600 μM 2,7-dichlorodihydrofluorescein diacetate (DCFH-DA; Santa Cruz Biotechnology; Gomes *et al. J. Biochem. Biophys. Methods* Vol. 65 (2005), 45). Signals are normalized by dividing by the baseline zero values. All samples were run in triplicate and error bars show standard deviations.

[0165] FIG. 7 show effective containment of MTALC in SAMP particles crucial for amplification was determined with a spin-filter test. The highly polar nature of MTALC, an anion, renders it challenging to comprise within a polymeric nanoparticle during aqueous washing. MTALC-comprising nanoparticles were fabricated using the method disclosed in US Provisional Application entitled "Water-inverted oil-oil nanoparticle formulation for hydrophilic species encapsulation", field on even date. Particles were dialyzed into 1x PBS and loaded into a microfuge spin-filter tube with a 20 kD membrane. Samples were spun and the filtrate was collected and tested for MTALC activity according to the procedure above. Each "wash" consists of particle resuspension into an addition of an equal amount of PBST and subsequent centrifugation and filtrate collection. Particles were "burst" using acetone followed by the addition of sodium bicarbonate buffer at pH 10. The baseline fluorescence reading is shown as a dashed line and labeled "baseline."

Example 6.

[0166] All genomic tests were conducted using a similar procedure. Genomic material was diluted 5-7 times in a 1:5 dilution series in 1x SSC buffer (Sigma-Aldrich) comprising 20 nM salmon sperm DNA (Sigma-Aldrich) and 0.001% Tween 20. Samples were heated for 5 min at 95°C to denature the DNA (note this step was not performed for RNA genomic material) and samples were cooled to 50°C. While at 50°C, magnetic capture microparticles (prepared as in Example 1) and TCO-Bz-Biot-comprising NPs (prepared as in Example 2), both functionalized with the appropriate primers, were added. The effective particle-bound primer concentrations were 2 μM. Samples were mixed for 30 minutes during the 50°C hybridization to prevent the microparticles from settling.

[0167] After hybridization, the samples were cooled to room temperature and washed 4 times with PBST using a magnetic stand for 1.5 mL-eppendorf tubes (Promega). The TCO-Bz-Biot crosslinker was released by adding a 1:1:1:1 solution of ethyl acetate : benzyl alcohol : ethanol : 0.1 M sodium hydroxide. Tetrazine-functionalized magnetic microparticles (prepared as in Example 1 using an amine-nonsense DNA-tetrazine primer from BioSynthesis) were then added in 1x PBS and the TCO-tetrazine reaction was allowed to proceed for 30 minutes at room temperature with shaking.

[0168] The particles were again washed 4 times with PBST on a magnetic capture stand and neutravidin at 1 μg/mL (ThermoFisher) was added in 1x PBS. This reaction proceeded for 30 minutes at room temperature with shaking.

[0169] The particles were again washed 4 times with PBST on a magnetic capture stand and biotin-functionalized MTALC-comprising SAMP particles (prepared as in Example 4) were added. The neutravidin-biotin reaction proceeded for 30 minutes at room temperature with shaking, after which the particles were washed 4 times with PBST on a magnetic capture stand. Acetone was then added to release the MTALC, followed by an equal-volume addition of 0.1 M bicarbonate buffer, with pipetting up-and-down performed between each step. An equal volume of 30 μM hydrogen peroxide and 600 μM DCFH-DA in 0.1 M bicarbonate buffer was then added. The tubes were placed back on the magnetic capture stand and the supernatant was transferred to a microplate and read at an excitation of 490 nm and an emission of 530 nm with a Molecular Devices M2 platereader.

Example 7.

[0170] Lettuce samples were prepared according to the procedure of Berrada *et al. Int. J. Food Microbiol.* Vol. 107 (2006) 202. Commercially-purchased romaine lettuce was homogenized in a 1:2 (w/w) ratio with deionized water for 5 minutes at 5,000 rpm (IKA). The resulting suspension was filtered first through a 0.8 μm and subsequently through a 0.2 μm syringe filter. *Listeria Monocytogenes* were cultured according to ATCC, Inc. instructions using agar plates with ATCC® Medium 44 Brain Heart Infusion Agar/Broth. *L. Monocytogenes* colonies were transferred from the plates to 1x SSC buffer and a serial dilution of bacteria in 1x SSC buffer was added to 4 filtered samples. Each sample was sonicated for 10 minutes (Heat Systems – Ultrasonics, Inc) and then treated at 95°C for 15 minutes in order to inactivate the bacteria. The samples were cooled to 50°C and the procedure from Example 6 was then followed for the remainder of the test.

Example 8.

[0171] The split flow multiplexing chip was designed in-house and the CAD layout is shown in Figure 12. The chip was fabricated by A-Line, Inc. The design consists of a 50 mm channel with two equal channels at both the inlet and outlet, each of which is

addressable individually with a hose barb connection. Each inlet was fitted with 1/16" ID silicone tubing fed by a syringe loaded in a syringe pump (Harvard Apparatus). One syringe was filled with the solution comprising mixed *Yersinia Pestis* and Dengue samples after the completion of the 50°C hybridization step. The second syringe was filled with 1x SSC buffer. The exit ports of the chip were fitted with similar tubing comprising valves, which allowed flows to be set. The tubing and plastic chip were treated with bovine serum albumin to minimize binding. A N52-grade neodymium magnet bar magnet (K&J Magnetics) was positioned ~2/3 the distance down the channel (from inlet to outlet). This was tuned empirically, together with syringe pump flow rates, such that 2 μm magnetic particles would traverse laterally across the channel, while 200 nm magnetic particles would remain in their original channel region. Upon completing of split flow fractionation, the *Y. Pestis* and Dengue samples were returned to 1.5 mL Eppendorf tubes and PBST washing was performed on the magnetic capture stand, followed by the release of the TCO-Bz-Biot crosslinker. The remainder of the procedure in Example 6 was then continued.

Example 9.

[0172] FAMP particles designed for protein binding were synthesized with TCO-Bz-Biot (Conju-Probe) as the payload and poly(*L*-lactic acid) (PLA; 500 kDa; PolySciTech) as the matrix forming agent. In order to confer biotin functionality to the particle surface, 1,2-distearoyl-sn-glycero-3-phosphoethanolamine-*N*-[biotinyl(polyethylene glycol)-2000] (DSPE-PEG-biotin; Laysan Bio) was used as the surfactant to stability the oil-in-water emulsion. These materials were dissolved in 2 mL chloroform in a 1:10:2 mass ratio. The resulting solution was then added to chloroform-saturated deionized water (0.815% chloroform in water) comprising 0.1% sodium dodecyl sulfate. The suspension was homogenized at 7,500 rpm (IKA) forming a milky, stable suspension, and was then processed with a Microfluidics LM 10microfluidizer at 3000 psi. This was subsequently added to a >300 mL solution of water, which clarified the solution. After clarification the particle solution was filtered through a 300 kD membrane (Millipore). The particles were concentrated to ~10 mL and stored in DI.

Example 10.

[0173] The assay for hCG was performed using the components of a commercially-available microplate ELISA kit (Ray Biotech). In order to bind released crosslinkers, a Nunc Maxisorp microplate was coated with tetrazine-functionalized bovine serum albumin (Tz-BSA). Tz-BSA was prepared by reacting NHS-Tz (Conju-Probe) with BSA for 2 hours at room temperature in PBS, pH 7.5, followed by overnight dialysis with a 3,000 MW cutoff membrane into PBS, pH 7.2. The coating of the microplate was performed in sodium bicarbonate buffer, pH 8.5, with BSA-Tz at 200 ng/mL.

Example 11.

[0174] Coated plates were incubated with 1/3-dilutions of the recombinant hCG standard. Four dilutions of the standard beyond the lowest dilution recommended in the kit instructions were used. After 2 hour room temperature binding followed by washing, the biotinylated detection antibody was added per the kit instructions. Following washing, for the "FAMP" group samples, a solution of 100 ng/mL neutravidin in assay diluent buffer "A" was added and allowed to bind for 1 hour. After washing the biotinylated FAMP nanoparticles were added in assay diluent buffer "A" and binding proceeded for 1 hour. After washing, a burst solution consisting of 10:0.8:0.1:0.1 of 0.1 M NaOH:ethanol:benzyl alcohol:ethyl acetate was added. The solution was then added to the BSA-Tz-coated microplate and binding was allowed to proceed for 1 hour at room temperature. Following washing, the streptavidin-HRP conjugate provided in the kit was added. Washing, 20 minute TMB development, and stop solution addition then proceeded reading the wells at 450 nm absorbance. For the "HRP control" group samples, following washing after biotinylated antibody binding, the streptavidin-HRP conjugate was then added per the kit instructions, followed by subsequent washing. After 30 minute TMB development and stop solution addition, the wells were read at 450 nm absorbance.

Example 12.

[0175] FIG. 8 shows specific detection of *Listeria Monocytogenes* genomic DNA (obtained from ATCC, Inc.) was achieved with the cascaded-amplification process using primers specific for 16S rDNA genes. The specific sequences were 5'-CTA TCC ATT GTA GCA CGT

G -modifiers-3' (SEQ ID NO:2) and 5'-modifiers-AGA ATA GTT TTA TGG GAT TAG-3' (SEQ ID NO:1) (Wang *et al. Appl. Environ. Microbiol.* Vol. 58 (1992), 2827). The number of copies of DNA was determined by quantitative PCR and 1:5 dilutions (v/v) were performed in 1x SSC buffer. Cascaded amplification was able to distinguish ~100 genomic copies. The zero point (no *L. Monocytogenes* DNA) is labeled as "0" and shown as a dashed line but is at "1" on the horizontal axis due to the log plot nature.

[0176] FIG. 9 shows specific detection of Dengue synthetic RNA (obtained from ATCC, Inc.) was achieved with the cascaded-amplification process using primers given by ATCC. The specific sequences were 5'-TGA GTG CGT GTG TCC AGT CC-modifiers-3' (SEQ ID NO:6) and 5'-modifiers-CAT GTC TCT ACC TTC TCG ACT TGT CT-3' (SEQ ID NO:7) (Gijavanekar *et al. FEBS J.* Vol. 278 (2011), 1676). The number of copies of the synthetic RNA genome was determined by quantitative PCR and 1:5 dilutions (v/v) were performed in 1x SSC buffer. Cascaded amplification was able to distinguish ~250 genomic copies directly from the RNA. The zero point (no Dengue RNA) is labeled as "0" and shown as a dashed line but is at "1" on the horizontal axis due to the log plot nature.

[0177] FIG. 10 shows specific detection of *Yersinia Pestis* genomic DNA (obtained from ATCC, Inc) was achieved with the cascaded-amplification process using the primers 5'-GAG GTC AGT GCT GCA TCA CC-modifiers-3'(SEQ ID NO:8) and 5'-modifiers-GCT CAG ATT TTG CCT GCA AA-3' (SEQ ID NO:9) specific for the *IS*100 element (Motin *et al. J. Bacteriol.* Vol. 184, (2002), 1019). The number of copies of the genomic DNA was determined by quantitative PCR and 1:5 dilutions (v/v) were performed in 1x SSC buffer. Cascaded amplification was able to distinguish ~300 genomic copies. The zero point (no *Y. Pestis* DNA) is labeled as "0" and shown as a dashed line but is at "1" on the horizontal axis due to the log plot nature.

[0178] FIG. 11 shows specific detection of *Listeria Monocytogenes* bacteria was performed in spiked lettuce samples. The Kim *L. Monocytogenes* strain was purchased from ATCC, Inc. and cultured with ATCC Medium 44. Lettuce samples were prepared according to the procedure of Berrada *et al. Int. J. Food Microbiol.* Vol. 107 (2006) 202. Briefly, store-bought romaine lettuce was homogenized and the resulting suspension was filtered through a 0.2 μm syringe filter. A serial dilution of bacteria was added to 4 filtered

samples. Cascaded amplification was able to distinguish ~250 colony forming units (CFUs).

[0179] FIGS. 12A-12C shows a schematic of magnetic fractionation device (1201) (**FIG.12A**) and fluorescence micrographs of red channel-active magnetic particles 2.85 μm in diameter (1202) (**FIG.12B**) and green channel-active particles 0.86 μm in diameter (1203) (**FIG.12C**). (Note the red channel-active particles bleed into the green channel.) The red particles moved across the channels in response to a bar magnet whereas the green particles were not sufficiently influenced to move. This device is a type of field-flow fractionation known as split flow thin-cell fractionation (Giddings *et al. Science* Vol. 193 (1976) 1244). Fluorescent microparticles were purchased from Bangs; red fluorescent magnetic particles were 2.85 μm diameter and green fluorescent magnetic particles were 0.86 μm diameter. This design permits magnetic particles of different sizes to be separated into two distinct solutions. This is one method for multiplexing cascaded amplification assays.

[0180] FIG. 13 shows a multiplexed *Y. Pestis* and Dengue test was performed at the highest dilution. The multiplexed points are circled (1301 is Dengue and 1302 is *Y. Pestis*). The data for *Y. Pestis*-alone and Dengue-alone is plotted on the same graph for comparison. This demonstrates the multiplexing capability of the cascaded amplification assay.

[0181] FIG. 14 shows a comparison of human chorionic gonadotropin (hCG) detection with standard ELISA ("HRP") and with FAMP particle binding and recruiting agent release followed by HRP signal generation ("FAMP"). The FAMP process permits sensitivities >50-fold greater than HRP alone.

Example 13.

Crosslinker Amplifier Nanoparticles

[0182] Initially, reactive small molecule crosslinkers were encapsulated in a polymer nanoparticle functionalized with specific ligands (**FIG. 15A**).

[0183] Although tyramide signal amplification is commercially available, reproducibility issues owing to the short-lived activated crosslinker and tyrosine concentration variations have limited its use (References *30, 31*). The reproducibility issue was

overcome here by utilizing nanolabels that encapsulate biotin-*trans*-cyclooctene (TCO) heterobifunctional crosslinkers (**FIG. 3**). When released upon triggered crosslinker-amplifier nanoparticle ("CAN") degradation ("burst"), the TCO groups rapidly bound surface tetrazine (Tz) groups, which are biologically inert and can thus be surface functionalized at a constant density, **FIG. 15B** (Reference *32*). Crosslinker binding conferred biotin functionality to the surface, which permitted binding to streptavidin-HRP (SAv-HRP) conjugates introduced in a following step. CAN amplification enhancement was determined by the number of encapsulated crosslinkers, whereas reproducibility was assessed by CAN uniformity. Functionalized CANs were formulated using microfluidizer-based shearing of an oil-in-water emulsion, which has been shown to scalably produce highly uniform polymeric nanoparticles (References *26,27*). This technique encapsulated $2x10^5$ crosslinkers per ~115 nm diameter CAN and yielded reproducible batches with low, <0.12 polydispersity indices (PDIs; **FIG. 4**).

[0184] CAN performance was first evaluated in comparison with a commercial *β*-human chorionic gonadotropin (*β*-hCG) ELISA. Standard and CAN-enhanced ELISAs were run in parallel, after the CAN-plate had been blocked with Tz-conjugated BSA. As shown in **FIG. 15C**, the CAN enhancement step produced a >100-fold sensitivity gain for the same endpoint absorbance reading. This permitted resolution of *β*-hCG levels in *in vitro* fertilization (IVF) embryo culture media, which requires ultra-sensitivities because of small, <20 µL sample volumes. A control sample, to which no embryo had been added, showed 17.3 ± 1.7 pg/mL *β*-hCG levels, whereas a sample from an embryo that grew for 5 days gave 76.4 ± 3.1 pg/mL *β*-hCG levels. Achieving such differentiation may be important for improving embryo transfer success rates for patients undergoing IVF and shows good agreement with previous results (References *33, 34*).

[0185] Another assessment of CAN performance in comparison to tyramide-amplified ELISA was carried out using human samples. The data in **FIG. 15D** show that CANs offer ~10-fold greater sensitivities than the tyramide baseline for IL-6 detection. CANs gave similar results to tyramide amplified ELISAs across multiple sample types, including human plasma samples and IVF embryo culture media (**FIG. 15E**). The enhanced resolution of the CAN "booster" could permit embryo growth to be tracked by IL-6 levels (Reference *33*).

Synthetic Amplifier Labels

[0186] Synthetic amplifier labels ("SALs") each comprise >10^4 densely packed small molecule catalysts shielded by a polymer shell functionalized with specific ligands (**FIG. 16A**). Similarly to CANs, SALs are chemically triggered to release their contents into solution after binding, permitting homogeneous catalysis of the optical signal. This design overcomes the diffusion problem inherent to surface-bound, heterogeneous catalysis, which reduces HRP performance to 5-14% that of its solution-phase activity (Reference *20*).

[0187] One of the fastest-known classes of aqueous-stable catalysts are iron-comprising tetra-amino metalorganic ligand, "TAML®," catalysts developed for green chemistry oxidation (References *28,29*). TAML compares very favorably to HRP, with molar activities within 5-fold those of this ELISA-standard enzyme, **FIG. 16B** (*2,3*). Thus, TAML represents a catalyst with near-enzyme kinetics. Furthermore, its small (<600 g/mol) molecular weight renders it ideal for nanoparticle encapsulation.

[0188] However, TAML is a charged, small molecule and is can pose challenges for encapsulation using standard emulsion nanoparticle formulation techniques (*18,19,35*). A new route for efficiently encapsulating high TAML loadings in functionalized nanoparticles can be used. This was achieved by designing a strategy that exploits TAML's hydrophilicity to trap it within the polar dispersed phase of an oil-in-oil emulsion, **FIG. 16C** (Reference *36*). TAML was then sealed within these cores by *in situ* polymerization, which occurs as the nanoparticles are precipitated into an aqueous phase (**FIG. 16D**). SALs produced with this reproducible, scalable process showed <0.15 PDIs (**FIG. 20**) and encapsulated >6×10^4 TAML molecules. These SALs were shelf-stable, producing similar amplifications after being stored for 4+ months at room temperature (**FIG. 21**), which is important for POC applications (Reference *37*).

[0189] SAL performance was compared against HRP for a *Clostridium difficile* Toxin A ELISA. *C. difficile* is now the leading cause of hospital-acquired infections and conventional *C. difficile* toxin ELISAs have poor LoDs that compromise efficient diagnoses (Reference *37*). SALs achieved >50-fold sensitivity enhancements over conventional *C. difficile* ELISAs (**FIG. 16E**). Furthermore, these *C. difficile* SAL results were similar to those achieved

using the highest-sensitivity immunoassay platform currently available, digital ELISA (References *14,38*). Digital ELISA showed a LoD of 0.028 pg/mL for *C. difficile* toxin A (*38*), compared with the 0.021 pg/mL LoD obtained for the SAL platform.

CAN-SAL Cascade

[0190] Enzyme replacement with nanolabels could remove one of the biggest barriers to PCR, the complex sample preparations required (References *5,39,40*). By utilizing CAN and SAL nanoparticles in series (**FIG. 17A**), PCR-like sensitivities are theoretically possible (**FIG. 17B**). As illustrated in **FIG. 17A**, CANs are functionalized with oligos complementary to specific template strands. After CANs and oligo-functionalized magnetic beads bind template strands, **FIG. 17A**(i), unbound CANs are washed away by magnetic capture. This design provides similar dual-primer specificity to PCR. Bound CANs are then burst, **FIG. 17A**(ii), releasing the crosslinkers and conferring biotin functionality to the magnetic beads, **FIG. 17A**(iii). This permits SAv-functionalized SALs to bind. SAL bursting then releases TAML to produce an optical signal, **FIG. 17A**(iv).

[0191] Low-level detection of *Lysteria monocytogenes* in real-time in food processing plants is important for detecting contamination before food is delivered to consumers (*41,42*). However, the complex sample preparations required by PCR often prevent its use in such settings, permitting contamination events to go unnoticed. CAN-bound oligos were thus first designed to bind *L. monocytogenes* DNA. In order to permit accurate comparisons with PCR, CANs were designed for stability at 50°C, which was chosen as the hybridization temperature. Measurements of CAN diameter (**FIG. 4**) and crosslinker release (**FIG. 22**) demonstrated CAN stability at 50°C. As shown in **FIG. 17C**, the CAN-SAL cascade had a LoD of ~100 template *L. monocytogenes* DNA strands. Importantly, the signal monotonically increased with template DNA strand concentration, suggesting the method is capable of quantification.

[0192] Lettuce homogenates represent a complex sample matrix important for *L. monocytogenes* detection in food processing plants (References *41,42*). The data in **FIG. 17D** were obtained by introducing oligo-functionalized CANs directly into lettuce homogenate samples. These results indicate that CAN-SAL is capable of detecting <20 specific DNA sequences directly from complex matrices. The enhanced LoD of **FIG. 17D**

relative to **FIG. 17C** is due to the use of CANs functionalized with multiple oligo sequences, each of which binds different, specific regions of the template strand (**FIG. 23**).

[0193] A direct comparison of CAN-SAL DNA detection in buffer and "complex media" comprised of heat-treated human plasma together with salmon sperm is given in **FIG. 18A**. These data show that CAN-SAL produced dose-dependent results for both sample types. Interestingly, LoDs for *L. monocytogenes* DNA in complex media were improved beyond those of buffer.

Silicon Photomultipler POC Detector

[0194] The choice of optical detector is important for achieving high sensitivity. In most laboratory applications, photomultiplier tubes (PMTs) are required in order to achieve low-signal precision and accuracy for fluorescence and chemiluminescence measurements (*43*). However, PMTs are expensive (~$2,000), bulky, and physically delicate and require >1 kV for operation. These constraints limit their application to the POC, where portability and robustness are critical (References *37,40,44*). Thus, current fluorescence POC devices often compromise sensitivity by replacing photomultiplier tubes (PMTs) ubiquitious in benchtop tools with photodiode detectors (References *40,44*).

[0195] A recent innovation in detection electronics, the silicon photomultiplier (SiPM), may permit PMT-quality data to be obtained with a small, portable detector. SiPMs are 1-10 mm^2 components comprised of a 2-D array of silicon avalanche photodiodes operating at a reverse bias of 30-70V in Geiger mode (Reference *45*). SiPMs have the further advantage of CMOS-compatibility, which permits easy integration with amplifier and processor chips. A detector prototype fabricated from SiPMs is shown in the inset in **FIG. 18B** that relies on photon counting, in which the SiPM signal is amplified with a high-speed transimpendance amplifier followed by a signal height discriminator and high speed counter. SiPMs permitted this portable detector to perform equivalent high-sensitivity fluorescence sensing to a state-of-the-art microplate reader incorporating PMTs (**FIG. 18B**).

[0196] This detector forms the basis of a microfluidic POC platform shown in **FIG. 24** that is designed for CAN-SAL cascade operation. The real-time SiPM-derived signals for two *L. monocytogenes* DNA samples are shown in **FIG. 18C**. These samples had the same DNA concentrations as the two points highlighted with arrows in **FIG. 18A** and showed similar results. The evolution of the signal from the low sample is clearly distinguished from that of the *L. monocytogenes* DNA-free control. These data demonstrate the ability of SiPMs to break the traditional tradeoff between sensitivity and portability.

Multiplexed Detection

[0197] Particularly in sample-constrained POC settings, multiplexed biomarker detection is important for maximal device utility (References *37,44*). The CAN-SAL cascade is easily adapted for multiplexing using the field flow fractionation (FFF) technique (Reference *46*) by using magnetic beads as the solid phase. In FFF, each analyte capture species is bound to a magnetic bead of a different size. As the mixed beads flow through a microfluidic channel, an external magnetic field draws the larger beads across the channel without affecting the smaller beads (**FIG. 19A**) achieving size-based separation (**FIG. 19B-C**).

[0198] The POC prototype was tested with FFF multiplexing with samples comprising a mixture of dengue RNA and *Yersinia pestis* DNA, causative agents of severe illnesses of global importance (References *47,48*). Reverse transcriptase is unnecessary due to the single DNA-RNA hybridization step necessary for detection. A dengue capture oligo was attached to 2 μm-diameter magnetic beads and a *Y. pestis* capture oligo to 200 nm-diameter beads. After hybridization and FFF, CAN-SAL assays were performed in parallel. **FIG. 19D** shows agreement between results obtained individually for dengue RNA or *Y. Pestis* DNA alone and those obtained simultaneously from the same sample, "multiplex." The slight gain in *Y. pestis* signal and corresponding loss in dengue signal was likely due to some 2 μm particles remaining in the original stream.

[0199] In order to counter the growing rise of bacterial antibiotic resistance, new therapeutics are being developed that target specific bacterial toxins, such as *S. aureus* α-hemolysin (α-Hla; References *49,50*). Simultaneous identification of *S. aureus* and α-Hla is thus important for maximizing utility of these next-generation therapies.

Pneumonia remains one of the most common serious infections caused by MRSA and exotoxigenic *S. aureus* (*51*). CAN-SAL was first evaluated for its ability to perform parallel identification of *S. aureus* (by rRNA) and MRSA (by *mecA*) on blinded clinical isolates. The data in **FIG. 25A** show that CAN-SAL produced equivalent results to PCR for genetic identification.

[0200] CAN-SAL was last used as a companion diagnostic to direct the new generation of toxin-specific antibiotic therapies (References *49,50*). This was achieved with multiplexed detection of α-Hla by SAL-immunoassay and *S. aureus* and MRSA by CAN-SAL cascade genetic identification. Isolates from seven human bronchiolar lavage (BAL) samples, the matrix routinely used clinically for diagnosis of pneumonia, were tested. The CAN-SAL cascade results for genetic identifiers were comparable to PCR for all samples (**FIG. 19E**). Importantly, the α-Hla assay indicated this toxin was present not only in all 3 MRSA samples, but in one of the non-MRSA S. aureus samples as well (**FIG. 19F**). This result would not have been identified had the samples been evaluated solely by PCR. The simulatenous recognition of the independent occurrence of exotoxin and antibiotic resistance demonstrates the power of multiplex protein and DNA detection.

Discussion

[0201] Biochemical binding events are commonly measured with amplifier labels. Some ultra-sensitive platforms engineer around the limitations of natural enzymes: two of note are intricate microfluidic and optical infrastructures that capture near-single molecule enzymatic effects (Reference *11*) and the coupling of polymerase activity with antibody detection (Reference *12*). More commonly, platforms engineer replacements for natural enzyme amplifiers.

[0202] Nanoparticles have demonstrated particular utility as amplifier labels and have been shown to extend LoDs over 2 orders of magnitude beyond ELISAs for proteins and achieve near-PCR levels of sensitivity for nucleic acids (References *7-9,13-17,20*). Achieving such ultra-sensitivities further benefits from adoption of new detection platforms: nanoparticle amplifier LoDs fall to ELISA-like levels when standard platereaders are used (References *22-25*). The present work demonstrates that

nanolabels can be designed for use with standard optical detection equipment but still achieve similar performance.

[0203] Advances in nanoparticle synthesis for targeted drug delivery have produced stable, reproducible formulations (References *18,19,35*). The present work adapts and expands on these to develop a new class of nanolabels that overcome reproducibility issues of current amplification schemes for optical assays (References *30,31,52,53*). The choice of TAML, a small-molecule catalyst with near-enzymatic kinetics, permits over 2 orders of magnitude more amplifiers to be encapsulated per particle compared with previous liposomal approaches (Reference *52*). These advances permit triggerable-nanolabels to enhance standard ELISA sensitivities by >100-fold and to quantify DNA and RNA with minimal sample preparation required.

[0204] The data presented herein demonstrate the feasibility of this approach for protein and nucleic acid assays. Ultra-sensitive detection of protein antigens is shown for different media for *β*-hCG (**FIG. 15C**), IL-6 (**FIG. 15D**), *C. difficile* toxin A (**FIG. 16E**), and *α*-Hla-toxin (**FIG. 19F**). These data are comparable to those from the highest-sensitivity platforms (References *7-9,14,38*). Quantitative detection of DNA and RNA, with a sensitivity approaching that of qPCR from complex samples, is demonstrated for, e.g., *L. monocytogenes* DNA (**FIG. 17C-D**, **FIG. 18A**), dengue RNA and *Y. pestis* DNA (**FIG. 19D**), and *S. aureus* rRNA and MSRA *mecA* DNA (**FIG. 17E**, **FIG. 25B**). Such LoDs are also comparable to the highest-sensitivity platforms (References *7-9,20*). Simultaneous detection of DNA/RNA and protein antigens provides a versatile platform that will facilitate development of biomarker panels as well as diagnostics in specific fields, such as infectious disease. The present example of multiplexed detection of MSRA and *α*-Hla toxin provides an opportunity to rapidly give clinicians information to optimize therapy and enhance patients outcomes through earlier treatment.

[0205] A key advance of the current approach using functionalized nanoparticles with reactive cargoes for macromolecule detection is that it couples homogeneous optical signal catalysis with a solid-phase binding assay. The solid-phase assay backbone maximizes specificity and selectivity (References *2,3*). Maximum sensitivity is then achieved by releasing catalysts from the solid surfaces into solution, where kinetics are

vastly improved. This design thus incorporates the best-known sensitivity, specificity, and catalytic paradigms and overcomes diffusion limitations that limit detection sensitivities of bound catalysts (References *20,28*).

[0206] Initially, to the surprise of the authors, detection of *L. monocytogenes* DNA appeared to have enhanced LoDs in complex samples compared with buffer (**FIG. 18A**). This finding was unexpected because complex samples comprising multiple species at varying concentrations often negatively affect assay sensitivities (References *7-9*). One possible explanation is that the mixture of species in complex samples is advantageous for reducing nanolabel nonspecific binding (NSB) in the present examples. Despite the promise of the triggerable nanolabel approach, experimental amplification factors are well below theoretical values, suggesting that LoDs are limited by factors such as NSB (References *53*).

[0207] The total amplification factor of the CAN-SAL cascade is the product of the number of crosslinkers per CAN (2×10^5) times the number of TAMLs per SAL (6×10^4) times the signal amplification of each TAML molecule. This theoretical product suggests that the method should give single-molecule sensitivity (**FIG. 17B**). In practice, however, single-oligo CAN-SAL has LoDs of 100 template strands, three orders of magnitude below the theoretical threshold. In addition to NSB, this may be due to nanolabels binding simultaneously to multiple adherent species or loss of nanolabels or small molecules during the washing steps. Increased understanding of the strength of the nanolabel binding to solid surfaces (*54*) and, in turn, optimizing washing will be important for achieving the technology's full potential. Additionally, developing improved TAML loading techniques for SALs can offer greater amplification factors.

[0208] Taken together, the findings disclosed herein suggest a novel platform for detection of diverse biomarkers using functionalized nanoparticles with reactive indicators sequestered in the inner compartment coupled with conventional optical detection equipment. Although further methodological optimization is likely, these results advance the field in a manner anticipated to accelerate collection of diagnostic and prognostic data to guide therapy.

[0209] The triggered-release of nanolabels developed in this work presents a powerful class of labels. Such nanolabels can provide broad access to high-performance assays and further offer the possibility of a single platform for multiple high-sensitivity biochemical assays. Furthermore, the approach is compatible with existing equipment, permitting researchers and clinical labs to achieve cutting-edge sensitivities without purchasing new detection equipment. Combined with a novel fluorimeter design, which permits precise, accurate measurements using a low-cost, portable device, these nanolabels may further permit a new era of ultrasensitive POC biomarker detection.

Materials and Methods

[0210] *CAN formulation.* CAN particles were synthesized with the Biot-TCO crosslinker (Conju-Probe) as the payload and poly(*L*-lactic acid) (PLA; 500 kDa; PolySciTech) as the polymer matrix. A poly(lactic acid)-poly(ethylene glycol)-maleimide block co-polymer of 30 kD:5 kD size (PolySciTech) was used to confer thiol reactivity. These materials were dissolved in 2 mL chloroform (Sigma) in a 1:10:2 mass ratio. The resulting solution was then added to chloroform-saturated deionized water (0.815% chloroform in water) comprising 0.1% sodium dodecyl sulfate (Sigma). The suspension was homogenized at 7,500 rpm forming a milky, stable suspension that was subsequently added to >300 mL of water for clarification. Because of maleimide instability in aqueous solutions, pH of the water was titrated to ~5.0 with dilute hydrochloric acid. The particle solution was immediately filtered through a 300 kD membrane (Millipore), and CANs were concentrated to ~10 mL and characterized with DLS and NanoSight techniques.

[0211] For nucleic acid studies, CANs were reacted with 3'-thiol-terminated oligonucleotides (Integrated DNA Technologies). The oligo sequence comprised a complementary DNA sequence followed by two "C18" spacers, shown to be sufficient removal from nanoparticles for rapid binding (*16*), followed by a 3'-dithiol endcap. The thiol-maleimide reaction proceeded at room temperature for 2 h in 1x PBS, pH 7.2, with 0.1 M TCEP. Conjugation efficacy was determined by optical density absorbance readings at 280 nm with turbidity controls at 320 nm. Reacted particles were dialyzed into 1x SSC buffer with a Slide-A-Lyzer cassette (ThermoFisher) and stored at 4°C.

[0212] CAN particles designed for protein binding were synthesized as above, and DSPE-PEG-biotin was added to the initial oil-in-water emulsion. The remainder of the CAN fabrication proceeded similarly. In order to confer neutravidin functionality to the particle surface, particle concentration was determined such that the effective biotin concentration in 1x PBS, pH ~7.2 was 0.1 μM. Neutravidin (ThermoFisher) was added at a concentration of ~10 μM and binding was allowed to proceed at room temperature for 2 h followed by filtering and concentrating the resulting particles with a 300 kD membrane and storage in 1x PBS.

[0213] *β-hCG assay.* Assays for β-hCG were performed using components of a commercially-available microplate ELISA kit and commercial β-hCG antibodies (Ray Biotech). In order to bind released crosslinkers, a Nunc Maxisorp microplate was coated with tetrazine-functionalized bovine serum albumin (Tz-BSA, 200 ng/mL in sodium bicarbonate buffer, pH 9.6) and the β-hCG antibody (25 ng/mL). Tz-BSA was prepared by reacting NHS-Tz (Conju-Probe) with BSA (Sigma) for 2 h at room temperature in PBS, pH 7.2, followed by overnight dialysis with a 3 kD-cutoff membrane (ThermoFisher) into PBS, pH 7.2.

[0214] Coated plates were incubated with 1/3-dilutions of the recombinant β-hCG standard. Four dilutions of the standard beyond the lowest dilution recommended in the kit instructions were used. A 2 h binding period at RT was followed by washing and addition of the biotinylated detection antibody per the manufacturer's instructions. For the CAN group of samples, after washing, the plate was incubated for 1 h with a solution of neutravidin (100 ng/ml) in assay diluent buffer "A" . After subsuqent washing, biotinylated CAN nanoparticles in assay diluent buffer "A" were added and binding proceeded for 1 h. Following additional washing, the plate was incubated for 1 h at room temperature with burst solution, consisting of 10:0.8:0.1:0.1 of 0.1 M NaOH:ethanol:benzyl alcohol:ethyl acetate. Streptavidin-HRP conjugate provided in the kit was added, wells were washed, and TMB was developed for 20 min prior to the addition of a stop solution and absorbance measurements at 450 nm. For HRP controls, after binding of biotinylated antibody, streptavidin-HRP conjugate was added per the manufacturer's instructions. After 30 min of TMB development, stop solution was added and wells were read at 450 nm.

[0215] IVF embryo culture media samples (CSC media, Irvine Scientific) comprise human serum albumin (Irvine Scientific) per standard clinical practice at Boston IVF. Two de-identified samples were obtained under a Boston IVF IRB: one from a sample that comprised an embryo for 5 days (IVF 1) and a control sample without an embryo (IVF 2).

[0216] *IL-6 assay.* CAN particles were synthesized as described above. Assays for IL-6 were performed using components of a commercially-available microplate "high-sensitivity" ELISA kit (eBioscience) based on tyramide signal amplification and commercial IL-6 antibodies (R&D Systems). Plate coating was performed as described above for *β*-hCG, with the only difference that the IL-6 capture antibody was plated at 15 ng/mL. The CAN assays were performed as described above for *β*-hCG and the high-sensitivity IL-6 assay was performed per the manufacturer's instructions. Human plasma samples were purchased commercially de-identified (Discovery Life Sciences) and de-identified IVF embryo culture media samples were provided under an existing IRB of Boston IVF as described above.

[0217] *HRP - TAML catalytic comparison.* HRP (Sigma, type vi) was dissolved in sodium acetate buffer, pH 5.5 and activity was determined using commercial TMB solution (ThermoFisher). Absorbance was measured after addition of 1 M sulfuric acid at 450 nm. TAML® (GreenOx Catalysts) was dissolved in bicarbonate buffer, pH 10; activity was determined using 2,7-dichlorodihydrofluorescein diacetate (Santa Cruz Biotech) and read at 490 nm/545 nm (Ref. *55*). All measurements were made using a Molecular Devices SpectraMax M2 microplate reader.

[0218] *SAL formulation.* Poly(lactic acid)-diacrylate (20 kD; PolySciTech) and TAML were dissolved in acetonitrile (Sigma) in a 5:1 mass ratio. A solution of poly(maleic anhydride-*alt*-octadecane) (PMAOD; Sigma) in cyclohexane (Sigma) was prepared. Acetonitrile solution was then added and homogenized into the cyclohexane at 7,500 rpm (IKA), forming a stable, milky emulsion clarified by the addition of benzene (Sigma). 1,2-distearoyl-sn-glycero-3-phosphoethanolamine-*N*-[biotinyl(polyethylene glycol)-2000] (DSPE-PEG-biotin; Laysan Bio) was added followed by . homogenization into 5x-volume of deionized water, forming a stable, milky emulsion with water as the continuous phase. The suspension was loaded into a round-bottom flask fitted with a reflux

condenser, flushed with nitrogen, heated to 50°C and stirred at 400 rpm. The reaction proceeded for 2 h, after which heating ceased, and the suspension was decanted and stirred overnight in a chemical fume hood. The resulting particles were filtered and concentrated with a 300 kD membrane (EMD Merck) and measured by DLS (Malvern) and NanoSight (Malvern) techniques.

[0219] In order to confer neutravidin functionality to the particle surface, particle concentration was determined such that the effective biotin concentration in 1x PBS, pH ~7.2 was 0.1 μM. Neutravidin (ThermoFisher) was added at a concentration of ~10 μM and binding was allowed to proceed at room temperature for 2 h followed by filtering and concentrating the resulting particles with a 300 kD membrane and storage in 1x PBS.

[0220] *C. difficile Toxin A assay.* A monoclonal antibody pair for *C. difficile* Toxin A (Meridian Life Sciences; C6555M, C01677M, C01678M) was used for the ELISA and SAL assays. The capture antibody was bound to *N*-hydroxysuccinimyl (NHS)-ester activated magnetic beads (ThermoFisher) per the manufacturer's instructions. The detection antibody was biotinylated using sulfo-NHS-LC-biotin (ThermoFisher), and the coupling reaction was performed for 2 h at RT in 1x PBS, pH 7.5. Recombinant *C. difficile* Toxin A (R&D Systems) was used to prepare a standard curve from 1000 pg/mL to 0.017 pg/mL.

[0221] Immunoassays were performed in triplicate using polypropylene tubes and a magnetic stand (Promega) for bead immobilization during wash steps. After the wash, following binding of the detection antibody, the mixture in each tube was divided into two parts and either streptavidin-HRP (Abcam) or neutravidin-functionalized SALs was added. Streptavidin-HRP labeled assays were developed with TMB solution (Abcam), stopped with 1 M sulfuric acid (Abcam), and absorbance read at 450 nm. SALs were burst with acetone and a solution comprising hydrogen peroxide and 2,7-dihydrodichlorofluorescein diacetate in bicarbonate buffer (pH 10) was then added followed by fluorescence measurement at 490/545 nm.

[0222] *Magnetic bead conjugation and primer sequences.* NHS-ester-functionalized superparamagnetic microparticles and nanoparticles (magbeads) were purchased from Bioclone and Ocean Nanotechnology, respectively. Oligos terminated with a 3'-amino

modifier were purchased from IDT. Starting at the 5'-termini, these oligos comprised an amino modifier followed by two "C18" spacers followed by the oligo sequence.

[0223] Primers for *L. monocytogenes* DNA were (Ref. *56,57*).:

AGAATAGTTTTATGGGATTAG (SEQ ID NO:1);

CTATCCATTGTAGCACGTG (SEQ ID NO:2);

ACCTCGCGGCTTCGCGAC (SEQ ID NO:3);

GGCTCTAACTACTTGTAGGC (SEQ ID NO:4); and

ACTGGTACAGGAATCTCTAC (SEQ ID NO:5).

[0224] Primers for *dengue* RNA were (Ref. *47,58*):

TGAGTGCGTGTGTCCAGTCC (SEQ ID NO:6); and

CATGTCTCTACCTTCTCGACTTGTCT (SEQ ID NO:7).

[0225] Primers for *Y. pestis* DNA were (Ref. *48*):

GAGGTCAGTGCTGCATCACC (SEQ ID NO:8); and

GCTCAGATTTTGCCTGCAAA (SEQ ID NO:9).

[0226] Primers *for S. aureus* rRNA were:

CTTAATGATGGCAACTAAGC (SEQ ID NO:10); and

AAATCCGGATAACGCTTGC (SEQ ID NO:11).

[0227] Primers for *S. aureus mecA* were (Ref. *54*):

CTTAGTTCTTTAGCGATTGC (SEQ ID NO:12); and

TTATATTGAGCATCTACTCGT (SEQ ID NO:13).

[0228] Primers for *K. pneumoniae* were (Ref. *59*):

AGAGTGATCTGCTCATGAA (SEQ ID NO:14); and

GAATTCGTCATATTCGGCCGT (SEQ ID NO:15).

[0229] Non-sense oligos comprising both an amino and a tetrazine modifier, used for crosslinker binding, were purchased from Bio-Synthesis, Inc.

[0230] Oligo-particle conjugation was performed according to the Bioclone protocol using magbeads (200 mg/mL) and oligo (5 μg/mL) in suspension buffer. In brief, the sample

was vortexed, reacted overnight at 50°C, and a 50:1 molar ratio of non-tetrazine-comprising oligo-to-Tz-comprising oligo was used. After 12 h, beads were washed with Bioclone buffer using a magnetic separation stand and then with deionized water at 50°C. Particles were resuspended at 20 mg/mL in 1x SSC buffer and stored at 4°C until use. Optical density measurements of the oligo solution before and after reactions at 280 nm were used to confirm conjugation.

[0231] *L. monocytogenes genomic DNA assays.* Purified genomic *L. monocytogenes* DNA (ATCC, Inc. 19114D-5) was diluted 5-7-times in a 1:5 dilution series using 1x SSC buffer comprising salmon sperm DNA (20 nM; Sigma) and Tween 20 (0.001%). Samples were heated for 5 min at 95°C to denature DNA (note this step was not performed for RNA genomic material) and samples were cooled to 50°C. While at 50°C, magbeads, prepared as above, and CANs, each functionalized with the appropriate primer, were added. The effective particle-bound primer concentration was 2 μM. Samples were mixed for 30 min during the 50°C hybridization period, and then cooled to room temperature and washed 4 times with PBST. Biot-TCO crosslinker was released by adding a 1:1:1:1 solution of ethyl acetate : benzyl alcohol : ethanol : 0.1 M sodium hydroxide. Particles were again washed 4 times with PBST and neutravidin (1 μg/mL) was added in 1x PBS. The reaction proceeded for 30 min at room temperature, and particles were again washed 4 times with PBST followed by addition of biotin-functionalized SALs. The neutravidin-biotin reaction proceeded for 30 min at room temperature, after which the particles were washed 4 times with PBST. Acetone was then added to release TAML, followed by addition of burst solution, as described above. Tubes were placed back on the magnetic capture stand and supernatant was transferred to a microplate for reading.

[0232] *L. monocytogenes bacteria assays.* Lettuce samples were prepared according to a previously published procedure (*39*). Commercially-purchased romaine lettuce was homogenized in a 1:2 (w/w) ratio with deionized water for 5 min at 5,000 rpm. The resulting suspension was sequentially filtered through 0.8 μm and 0.2 μm syringe filters (VWR). *Listeria monocytogenes* (ATCC 19114) were cultured according to ATCC instructions using agar plates with ATCC® Medium 44 Brain Heart Infusion Agar/Broth. *L. Monocytogenes* colonies were transferred from plates to 1x SSC buffer and serial

dilutions of bacteria in 1x SSC buffer were added to four filtered samples. Each sample was sonicated for 10 min (Heat Systems – Ultrasonics, Inc) and then treated at 95°C for 15 min in order to kill bacteria. Samples were cooled to 50°C and the procedure described above was followed.

[0233] *Fractional Flow Filtration.* The fractional flow filtration chip was designed in-house and fabricated by A-Line, Inc. The design consists of a 5 mm x 50 mm channel with Y junctions at both inlet and outlet (2.5 mm), separated by 200 μm wide and 5 mm long divider to minimize fluid mixing at junctions and allow straight fluid lines. Each inlet was fitted with 1/16" ID and 1/8" OD silicone tubing fed by a syringe loaded onto a syringe pump (Harvard Apparatus). One syringe was filled with solution comprising a mixture of *Y. Pestis* and Dengue samples after completing hybridization at 50°C. A second syringe was filled with 1x SSC buffer. Exit ports were fitted with similar tubing comprising valves, which allowed flows to be set. Tubing and plastic chip were treated with BSA to minimize nonspecific binding. An N52-grade neodymium magnet bar magnet (K&J Magnetics) was positioned ~2/3 the distance down the channel (from inlet to outlet). The latter was tuned empirically, together with syringe pump flow rates, such that 2 μm magnetic particles would laterally traverse the channel, while 200 nm magnetic particles would remain in their original channel region.

[0234] *SiPM Fluorimeter.* An SiPM (Hamamatsu S13360-3050CS, 3 mm x 3 mm chip and 50 x 50 micrometer pixels) was biased at the appropriate reverse voltage above the specified breakdown voltage. The output from the SiPM was run thourgh a singal processing hardware taken from SP5600 unit made by CAEN S.p.A. which provides a variable gain amplifier, comaprator with a variable threshold voltage and a counter. A software was written for a National Instruments Data Acquisition Card to read datastreams and generate all control and synchronization signals for readout electronics, excitation Light Emitting Diode (LED, from LedEngin), pumps and valves. SiPM voltage bias, discriminator threshold and amplifier gain were adjusted to permit the highest sensitivity and dynamic range, and the lowest dark count for a reference fluorescent solution (100nM fluorescein, Sigma, in DI water). The emission LED was biased using an external circuit providing 250 ns pulses at 1 MHz frequency. Excitation pulse width and frequency were set to provide the highest signal-to-noise ratio for reference fluorescence solution.

Excitation (480 nm) and emission filters (530 nm) were purchased from Thorlabs. Optical system made of lenses, optical tubes and holders (Thorlabs) was used to focus light from microfluidic chip onto the SiPM and minimize stray light.

Microfluidic platform.

[0235] The microfluidic assay cartridge was designed in-house and manufactured by A-Line Inc. Fluid control was achieved by off-chip valves and a diaphragm pump (Takasago Fluidics). The pump was placed at the outlet thereby creating negative pressure. The cartridge consisted of 3 parallel channels that allow detection of 3 separate samples. Each channel consisted of 2 zones: one for assay incubation and other for detection. The assay zone was designed to fit a cylindrical (¼" diameter and ¼" height) N52 grade neodymium magnet to trap functionalized magnetic particles. Dettection zone of the chip was spotted with BSA-Tz to permit capture of Biotion-TCO from CAN. After spotting with BSA-TZ chips were sealed and channels were incubated with 1% BSA solution to minimize non-specific binding. Biotin-TCO released from CAN in the assay zone was moved to detection zone and incubated for 30 minutes, followed by a wash step. SALs were then introduced to detection zone and incubated for 20 minutes followed by a wash cycle. Release solution was then introduced and signal was measured in real-time using SiPM fluorometer. In order to achieve maximum photon collection, the detection zone was a 100µm thick layer made of cyclo olefin copolymer (COC) in order to minimize absorbance and auto-fluorescence.

[0236] **FIGS. 24A-24B** show microfluidic chip layouts. **FIG.24A** is an exploded view and **FIG. 24B** is a complete view of a microfluidic chip used for *L. monocytogenes* DNA detection. Up to three assays can be run on a same chip. Recesses in the top layer are for N52-grade niobium magnets and optical windows allow detection of optical signals.

[0237] *Dengue and Y. pestis assays.* Synthetic dengue viral RNA (VR-3230SD) and purified *Y. pestis* DNA (BAA-1608D-5) were purchased from ATCC. Samples were mixed at a known concentration and hybridization was performed as described for *L. monocytogenes* assays. The sample was then diluted 1:10 and loaded into a syringe fitted to a syringe

pump for FFF. Upon completion of FFF, the *Y. Pestis* and dengue samples were returned to 1.5 mL eppendorf tubes and loaded into the microfluidic assay chip.

[0238] *Microfluidic assays.* The sequence of steps followed those for *L. monocytogenes* detection, with a magnet positioned in a recess on the microfluidic platform used to hold magbeads during wash steps. One exception was that no tetrazine-comprising oligos were used on magbeads. Instead, Tz-BSA was spotted on the microfluidic chip surface. The small channel dimensions of microfluidic channels (300 μm wide and 500 μm high) ensured rapid kinetics. The signals were read by the SiPM fluorimeter.

[0239] *BAL sample preparation.* Commercial human BAL samples (Discovery Life Sciences) were streaked on LB agar plates (EZ BioResearch), inverted, and grown overnight at 35°C. These samples were chosen based on availability on a single day of clinical BAL samples and were numbered in the order they were removed from the sample bag. Five colonies from each plate were picked and resuspended in PBS.

[0240] *α-Hla assay.* Antibodies and the α-Hla protein standard were purchased from Abcam. The samples were incuabated with human IgG (1 μg/mL; Sigma) for 30 minutes and then the IgG-comprising samples were introduced for the capture step. This procedure was performed to minimize protein A interference. The remainder of the procedure for the α-Hla toxin assay was similar to that described for *C. difficile* toxin A.

[0241] *S. aureus and MRSA assays.* A RNA/DNA extraction kit (Qiagen QIAmp UCP Pathogen Mini Kit) was used to purify nucleic acid material from the pellets of the commercial human BAL samples according to the manufacturer's instructions. The remainder of the procedure was similar to that for *L. monocytogenes* assays. The PCR controls were performed using commercial Qiagen kits for the 16S rRNA gene (BBID00314; page AR) and the *mecA* gene (BBAR00374AR).

[0242] *Blinded sample testing.* Samples were provided "blinded" as 10 labeled 1.5 mL microfuge tubes (B1-B10) with no identifying information. Samples were produced by a collaborator at a different facility who maintained the sample key at the institution of origin. The CAN-SAL results were emailed to the collaborator when the assays were complete and the collaborator returned the results. No exchanges between assay

operators and the collaborator transpired between acknowledgement of sample delivery and sending the results email 2 days later.

[0243] References

1. O. Bahcall. Precision medicine. *Nature.* **526** (2015) 335.
2. R.M. Lequin. Enzyme immunoassay (EIA)/enzyme-linked immunosorbent assay (ELISA). *Clin. Chem.* **51**, 2415-2418 (2005).
3. Deshpande, S.S. (1996). *Enzyme Immunoassays: From Concept to Product Development*. New York, NY: Chapman & Hall.
4. P.M. Holland, R.D. Abramson, R. Watson, D.H. Gelfand. Detection of specific polymerase chain reaction product by utilizing the 5'----3' exonuclease activity of Thermus aquaticus DNA polymerase. *Proc. Nat'l. Acad. SAL.* **88**, 7276-7280 (1991).
5. M. Kubista, J.M. Andrade, M. Bengtsson, A. Forootan, J. Jonak, K. Lind, R. Sindelka, R. Sjoback, B. Sjogreen, L. Strombom, A. Stahlberg, N. Zoric. The real-time polymerase chain reaction. *Molec. Aspects Med.* **27**, 95-125 (2006).
6. K. Muzyka. Current trends in the development of the electrochemiluminescent immunosensors. *Biosens. Bioelectron.* **54**, 393-407 (2014).
7. S.O. Kelley, C.A. Markin, D.R. Walt, R.F. Ismagilov, M. Toner, E.H. Sargent. Advancing the speed, sensitivity and accuracy of biomolecular detection using multi-length-scale engineering. *Nature Nanotechnol.* **9**, 969-980 (2014).
8. D.A. Giljohann, C.A. Mirkin. Drivers of biodiagnostic development. *Nature*. **462**, 461-464 (2009).
9. H. Chandra, P.J. Reddy, S. Srivastava. Protein microarrays and novel detection platforms. *Expert Rev. Proteom.* **8**, 61-79 (2011).
10. H.K. Hunt, A.M. Armani. Label-free biological and chemical sensors. *Nanoscale.* **2**, 1544-1559 (2010).
11. D.M. Rissin, C.W. Kan, T.G. Campbell, S.C. Howes, D.R. Fournier, L. Song, T. Piech, P.P. Patel, L. Chang, A.J. Rivnak, E.P. Ferrell, J.D. Randall, G.K. Provuncher, D.R. Walt, D.C. Duffy. Single-molecule enzyme-linked immunosorbent assay detects serum proteins at subfemtomolar concentrations. *Nature Biotechnol.* **28**, 595-599 (2010).
12. C.M. Niemeyer, M. Adler, R. Wacker. Detecting antigens by quantitative immune-PCR. *Nat. Protoc.* **2**, 1918-1930 (2007).

13. J. Wang, R. Polsky, A. Merkoci, K.L. Turner. 'Electroactive beads' for ultrasensitive DNA detection. *Langmuir* **19**, 989-991 (2003).
14. J. Das, I. Ivanov, E.H. Sargent, S.O. Kelley. An electrochemical clamp assay for direct, rapid analysis of circulating nucleic acids in serum. *Nature Chem.* **7**, 569-575 (2015).
15. B.S. Munge, A.L. Coffey, J.M. Doucette, B.K. Somba, R. Malhotra, V. Patel, J.S. Gutkind, J.F. Rusling. Nanostructured immunosensor for attomolar detection of cancer biomarker interleukin-8 using massively labeled superparamagnetic particles. *Angew. Chem. Int. Ed.* **50**, 7915-7918 (2011).
16. H.J. Chung, C.M. Castro, H. Im, H. Lee, R. Weissleder. A magneto-DNA nanoparticle system for rapid detection and phenotyping of bacteria. *Nature Nanotechnol.* **8**, 369-375 (2013).
17. H. Harma, T. Soukka, T. Lovgren. Europium nanoparticles and time-resolved fluorescence for ultrasensitive detection of prostate-specific antigen. *Clin. Chem.* **47**, 561-568 (2001).
18. L. Gao, J. Zhuang, L. Nie, J. Zhang, Y. Zhang, N. Gu, T. Wang, J. Feng, D. Yang, S. Perrett, X. Yan. Intrinsic peroxidase-like activity of ferromagnetic nanoparticles. *Nature Nanotechnol.* **2**, 577-583 (2007).
19. S. Kumari, B.B. Dhar, C. Panda, A. Meena, S. Sen Gupta. Fe-TAML encapsulated inside mesoporous silica nanoparticles as peroxidase mimic: femtomolar protein detection. *ACS Appl. Mater. Interfaces* **6**, 13866-13873 (2014).
20. S. Rauf, D. Zhou, C. Abell, D.J. Kang. Building three-dimensional nanostructures with active enzymes by surface templated layer-by-layer assembly. *Chem. Commun.* **16**, 1721-1723 (2006).
21. C.P. Chan, Y. Bruemmel, M. Seydack, K.-k. Sin, L.-w. Wong, E. Merisko-Liversidge, D. Trau, R. Renneberg. Nanocrystal biolabels with releasable fluorophores for immunoassays. *Anal. Chem.* **76**, 3638-3645 (2004).
22. N. Bunyakul, K.A. Edwards, C. Promptmas, A.J. Baeumner. Cholera toxin subunit B detection in microfluidic devices. *Anal. Bioanal. Chem.* **393**, 177-186 (2009).
23. F. Mouffouk, Y. Chishti, Q. Jin, M.E. Rosa, M. Rivera, S. Dasa, L. Chen. Polymeric micelle-based bioassay with femtomolar sensitivity. *Anal. Biochem.* **372**, 140-147 (2008).

24. X. Shu, Y. Liu, J. Zhu. DNA detection based on fluorogenic nanospheres. *Angew. Chem. Int. Ed.* **51**, 11006-11009 (2012).

25. W. Qu, Y. Liu, D. Liu, Z. Wang, X. Jiang. Copper-mediated amplification allows readout of immunoassays by the naked eye. *Angew. Chem. Int. Ed.* **50**, 3442-3445 (2011).

26. M.D. Glasgow, M.B. Chougule. Recent developments in active tumor targeted multifunctional nanoparticles for combination chemotherapy in cancer treatment and imaging. *J. Biomed. Nanotechnol.* **11**, 1859-1898 (2015).

27. A.Z. Wang, R. Langer, O.C. Farokhzad. Nanoparticle delivery of cancer drugs. *Annu. Rev. Med.* **63**, 185-198 (2012).

28. S.S. Gupta, M. Stadler, C.A. Noser, A. Ghosh, B. Steinhoff, D. Lenoir, C.P. Horwitz, K.W. Schramm, T.J. Collins. Rapid total destruction of chlorophenols by activated hydrogen peroxide. *Science* **296**, 326-328 (2002).

29. T.J. Collins. TAML oxidant activators: a new approach to the activation of hydrogen peroxide for environmentally significant problems. *Acc. Chem. Res.* **35**, 782-790 (2002).

30. E.C. Stack, C. Wang, C.C. Hoyt. Multiplexed immunohistochemistry, imaging, and quantitation: a review, with an assessment of tyramide signal amplification, multispectral imaging and multiplex analysis. *Methods* **70**, 46-58 (2014).

31. Z. Gao, L. Hou, M. Xu, D. Tang. Enhanced colorimetric immunoassay accompanying with enzyme cascade amplification strategy for ultrasensitive detection of low-abundance protein. *Sci. Reports* **4**, 3966 (2014).

32. D.M. Patterson, L.A. Nazarova, J.A. Prescher. Finding the right (bioorthogonal) chemistry. *ACS Chem. Biol.* **9**, 592-605 (2014).

33. A. Bourdiec, E. Calvo, C.V. Rao, A. Akoum. Transcriptome analysis reveals new insights into the modulation of endometrial stromal cell receptive phenotype by embryo-derived signals interleukin-1 and human chorionic gonadotropin: possible involvement in early embryo implantation. *PLoS One* **8**, e64829 (2013).

34. C. Xiao-yan, L. Jie, J. Dang, L. Tao, L. Xin-Ru, Z. Guang-Lun. A highly sensitive electrochemiluminescence immunoassay for detecting human embryonic human chorionic gonadotropin in spent embryo culture media during IVF-ET cycle. *J. Assist. Reprod. Genet.* **30**, 377-382 (2013).

35. K. Cho, X.U. Wang, S. Nie, D.M. Shin. Therapeutic nanoparticles for drug delivery in cancer. *Clin. Cancer Res.* **14**, 1310-1316 (2008).

36. M. Klapper, S. Nenov, R. Haschick, K. Muller, K. Mullen. Oil-in-oil emulsions: a unique tool for the formation of polymer nanoparticles. *Acc. Chem. Res.* **41**, 1190-1201 (2008).

37. P.K. Drain, E.P. Hyle, F. Noubary, K.A. Freedberg, D. Wilson, W.R. Bishai, W. Rodriguez, I.V. Bassett. Diagnostic point-of-care tests in resource-limited settings. *Lancet.* **14**, 239-249 (2014).

38. L. Song, M. Zhao, D.C. Duffy, J. Hansen, K. Shields, M. Wungjiranirun, X. Chen, H. Xu, D.A. Leffler, S.P. Sambol, D.N. Gerding, C.P. Kelly, N.R. Pollock. Development and validation of digital enzyme-linked immunosorbent assays for ultrasensitive detection and quantification of *Clostridium difficile* toxins in stool. *J. Clin. Microbiol.* **53**, 3204-3212 (2015).

39. C.J. Smith, A.M. Osborn. Advantages and limitation of quantitative PCR (Q-PCR)-based approaches in microbial ecology. *FEMS Microbiol. Ecol.* **67**, 6-20 (2009).

40. C.D. Chin, V. Linder, S.K. Sia. Commercialization of microfluidic point-of-care diagnostic devices. *Lab Chip.* **12**, 2118-34 (2012).

41. C. Ohshima, H. Takahashi, C. Phraephaisam, M. Vesaratchavest, S. Keeratipibul, T. Kuda, B. Kimura. Establishment of a simple and rapid identification method for *Listeria* spp. by using high-resolution melting analysis, and its application in food industry. *PLOS One.* **9**, e99223 (2014).

42. D. Bae, K.S. Seo, T. Zhang, C. Wang. Characterization of a potential *Listeria monocytogenes* virulence factor associated with attachment to fresh produce. *Appl. Environ. Microbiol.* **79**, 6855-6861 (2013).

43. F. Berthold, V. Tarkkanen. Luminometer development in the last four decades: recollections of two entrepreneurs. *Luminescence.* **28**, 1-6 (2012).

44. N.M.M. Pires, T. Dong, U. Hanke, N. Hoivik. Recent developments in optical detection technologies in lab-on-a-chip devices for biosensing applications. *Sensors*. **14**, 15458-15479 (2014).

45. F. Meddi, F. Ambrosino, R. Nesci, C. Rossi, S. Sclavi, I. Bruni, A. Ruggeri, S. Sestito. A new fast silicon photomultiplier photometer. *Astronom. Soc. Pacific.* **59**, 448-453 (2012).

46. K.E. Herold & A. Rasooly, Eds. *Lab on a Chip Technology: Biomolecular Separation and Analysis*. (Caister Academic Press, Norfolk, UK, 2009).

47. C. Gijavanekar, M. Añez-Lingerfelt, C. Feng, C. Putonti, G.E. Fox, A. Sabo, Y. Fofanov, R.C. Willson. PCR detection of nearly any dengue virus strain using a highly sensitive primer 'cocktail.' *FEBS J.* **278**, 1676-1687 (2011).

48. V.L. Motin, A.M. Georgescu, J.M. Elliott, P. Hu, P.L. Worsham, L.L. Ott, T.R. Slezak, B.A. Sokhansanj, W.M. Regala, R.R. Brubaker, E. Garcia. Genetic variability of *Yersinia pestis* isolates as predicted by PCR-based IS*100* genotyping and analysis of structural genes encoding glycerol-3-phosphate dehydrogenase (*glpD*). *J. Bacteriol.* **184**, 1019-1027 (2002).

49. J. Bubeck Wardenburg, O. Schneewind. Vaccine protection against *Staphylococcus aureus* pneumonia. *J. Exp. Med.* **205**, 287-24 (2008).

50. G.R. Sampedro, A.C. DeDent, R.E. Becker, B.J. Berube, M.J. Gebhardt, H. Cao, J. Bubeck Wardenburg. Targeting *Staphylococcus aureus* α-toxin as a novel approach to reduce severity of recurrent skin and soft-tissue infections. *J. Infect. Dis.* **210**, 1012-1018 (2014).

51. F.R. DeLeo, B.A. Diep, M. Otto. Host defense and pathogenesis in *Staphylococcus aureus* infections. *Infect. Dis. Clin. North Am.* **23**, 17-34 (2009).

52. S.Y. Hwang, Y. Kumada, G.H. Seong, J. Choo, S. Katoh, E.K. Lee. Characteristics of a liposome immunoassay on a poly(methyl methacrylate) surface. *Anal. Bioanal. Chem.* **389**, 2251-2257 (2007).

53. D.A. Hendricks, L. Comanor (2006). Signal Amplification-Based Techniques. In *Nucleic Acid Testing for Human Disease*, A. Lorincz *Ed.* Boca Raton, FL: Taylor & Francis Group.

54. C. Tassa, J.L. Duffner, T.A. Lewis, R. Weissleder, S.L. Schreiber, A.N. Koehler, S.Y. Shaw. Binding affinity and kinetic analysis of targeted small molecule-modified nanoparticles. *Bioconj. Chem.* **21**, 14-19 (2010).

55. A. Gomes, E. Fernandes, J.L.F.C. Lima. Fluorescence probes used for detection of reactive oxygen species. *J. Biochem. Biophys. Meth.* **65**, 45-80 (2005).

56. A. Bubert, I. Hein, M. Rauch, A. Lehner, B. Yoon, W. Goebel, M. Wagner. Detection and differentiation of *Listeria* spp. by a single reaction based on multiplex PCR. *Appl. Environ. Microbiol.* **65**, 4688-4692 (1999).

57. J.-U. Kim, C.-H. Cha, H.-K. An, H.-J. Lee, M.-N. Kim. Multiplex real-time PCR assay for detection of methicillin-resistant *Staphylococcus aureus* (MRSA) strains suitable in regions of high MRSA endemicity. *J. Clin. Microbiol.* **51**, 1008-1013 (2013).

58. http://www.atcc.org/products/all/VR-3230SD.aspx#documentation. Accessed 15 Mar 2016.

59. R.J. Clifford, M. Milillo, J. Prestwood, R. Quintero, D.V. Zurawski, Y.I. Kwak, P.E. Waterman, E.P. Lesho, P. McGann. Detection of bacterial 16S rRNA and identification of four clinically important bacteria by real-time PCR. *PLOS One.* **7**, e48558 (2012).

[0244] All publications and patent applications cited in this specification are hereby incorporated by reference herein in their entireties as if each individual publication or patent application were specifically and individually indicated as being incorporated by reference and as if each reference was fully set forth in its entirety. To the extent that there is any conflict between any publication or patent application incorporated herein, the present specification controls. Although the foregoing invention has been described in some detail by way of illustration and example for purposes of clarity of understanding, it will be readily apparent to those of ordinary skill in the art in light of the teachings of this invention that certain changes and modifications may be made thereto without departing from the spirit or scope of the appended claims.

Claims

1. A method of detecting one or more analytes in a sample comprising:

incubating a sample with a plurality of nanoparticles comprising one or more payloads comprising one or more recruiting agents, wherein each nanoparticle is functionalized with moieties enabling specific binding of an analyte and a plurality of capture particles is functionalized with moieties capable of binding the same analyte;

releasing the one or more recruiting agents from the nanoparticles bound to the analytes;

introducing a plurality of catalyst-comprising particles, each comprising one or more functionalities capable of specifically binding to the recruiting agent;

dissociating the catalyst-comprising particles bound to the recruiting agents thereby generating signals; and

determining the presence or quantity of the analyte in the sample based on the generated signals.

2. The method of claim 1, where the analyte to be detected is a nucleic acid, a protein, a small molecule, an organism, or a virus.

3. The method of claim 2, wherein the analyte to be detected is a nucleic acid.

4. The method of claim 3, wherein the nucleic acid is a DNA or RNA.

5. The method of any one of claims 1-4, wherein the moieties on the recruiting agent-comprising nanoparticles and the capture particles bind one or more different regions of the analyte to be detected.

6. The method of any one of claims 1-5, wherein the recruiting agent-comprising nanoparticles and the capture particles each fall into the size range of 25 nm to 10 microns (e.g., 25 nm to 1 micron, 25 nm to 500 nm, 25 nm to 250 nm, or 25 nm to 100 nm).

7. The method of any one of claims 1-6, wherein the recruiting agent-comprising nanoparticles comprise an enzyme conjugate to facilitate signal generation.

8. The method of claim 7, wherein the enzyme is HRP, AP, and/or ACE.

9. The method of any one of claims 1-8, wherein the capture particles are susceptible to an external magnetic, optical, and/or acoustic field and/or a size exclusion gradient.

10. The method of any one of claims 1-9, wherein the recruiting agents are chemical and/or biochemical crosslinkers, comprising one or more of the same or different functional moieties.

11. The method of any one of claims 1-10, wherein the catalyst-comprising species is one or more of particulate, enzymatic, and/or polymeric in nature.

12. The method of any one of claims 1-11, wherein the generated signal is optical and/or electronic.

13. The method of any one of claims 1-12, wherein the particles bound to the analytes are addressable.

14. The method of claim 13, wherein the addressable particles are susceptible to different fields and/or gradients such that multiple analytes are detected in parallel.

15. The method of any one of claims 1-14, wherein the method comprises mixing steps to prevent settling of the particles.

16. The method of any one of claims 1-15, wherein the method is performed in a glass, polymeric, or metallic vessel and/or microfluidic platform.

17. The method of any one of claims 1-16, wherein the moieties on the recruiting agent are bound to a solid support.

18. The method of claim 17, wherein the solid support is a particle susceptible to an external magnetic, optical, and/or acoustic field and/or a size exclusion gradient.

19. The method of any one of claims 1-18, wherein a sample pre-treatment is performed prior to the onset of the assay.

20. The method of any one of claims 1-19, wherein one or more of the moieties specific for the analytes to be detected is not functionalized to the recruiting agent-comprising nanoparticles and/or capture particles at the time of binding but, rather, binds one or more of these particle types after binding the analyte to be detected.

21. The method of any one of claims 1-20, wherein the recruiting agent reacts with the catalyst-comprising particles to expose the catalyst.

22. The method of any one of claims 1-21, wherein the method comprises adding one or more additional recruiting agent-comprising nanoparticles for multi-tiered amplification.

23. The method of any one of claims 1-22, wherein the recruiting agent-comprising nanoparticles or the catalyst-comprising particles do not comprise protein signal precursor molecules and/or carrier protein.

24. A kit for detecting one or more analytes in a sample comprising:

a plurality of nanoparticles comprising one or more payloads comprising one or more recruiting agents, wherein each nanoparticle is functionalized with moieties enabling specific binding of an analyte;

a plurality of capture particles functionalized with moieties capable of binding the same analyte;

a solution for releasing the one or more recruiting agents from the nanoparticles; and

a plurality of catalyst-comprising particles, each comprising one or more functionalities capable of specifically binding to the recruiting agent; and

a solution comprising reagents for performing a reaction that generates signals, once the catalyst is released.

25. The kit of claim 24, wherein the recruiting agent-comprising nanoparticles and the capture particles each fall into the size range of 25 nm to 10 microns (e.g., 25 nm to 1 micron, 25 nm to 500 nm, 25 nm to 250 nm, or 25 nm to 100 nm).

26. The kit of claim 24 or claim 25, wherein the recruiting agent-comprising nanoparticles comprise an enzyme conjugate to facilitate signal generation.

27. The kit of claim 26, wherein the enzyme is HRP, AP, and/or ACE.

28. The kit of any one of claims 24-27, wherein the recruiting agents are chemical and/or biochemical crosslinkers, comprising one or more of the same or different functional moieties.

29. The kit of any one of claims 24-28, wherein the catalyst-comprising species is one or more of particulate, enzymatic, and/or polymeric in nature.

30. The kit of any one of claims 24-29, wherein the kit further comprises a glass, polymeric, or metallic vessel and/or microfluidic platform.

31. The kit of any one of claims 24-30, wherein the kit further comprises a solid support.

32. The kit of any one of claims 24-31, wherein the recruiting agent-comprising nanoparticles or the catalyst-comprising particles do not comprise protein signal precursor molecules and/or carrier protein.

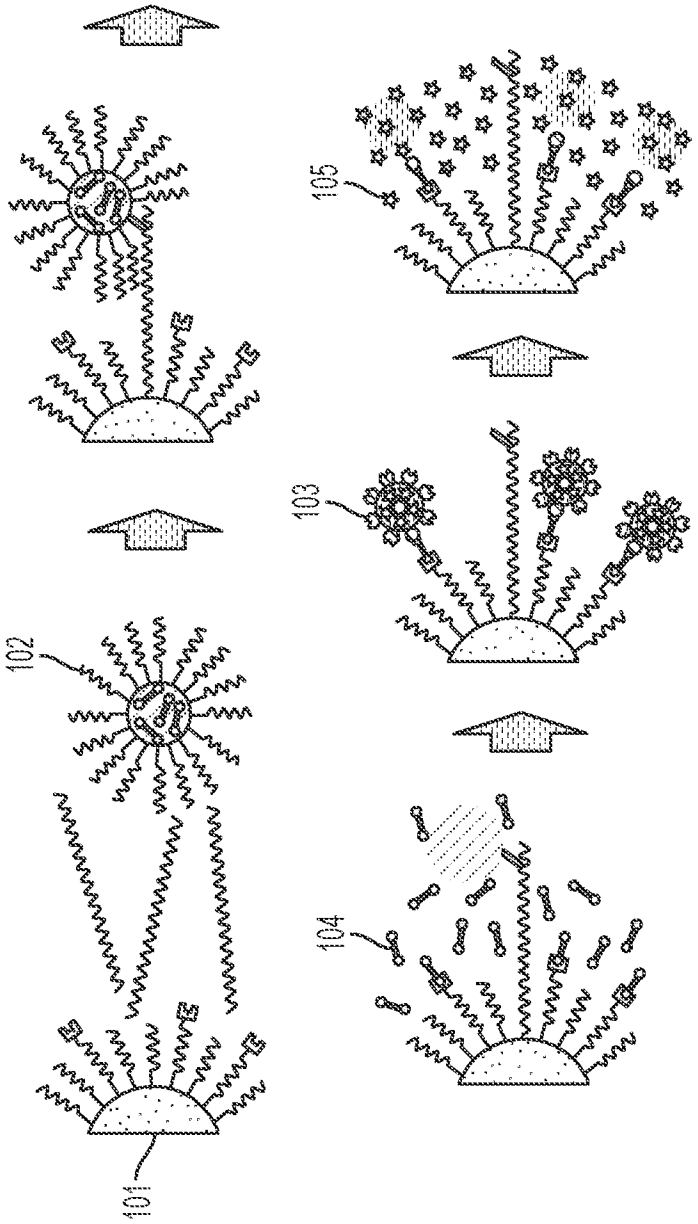


FIG. 1

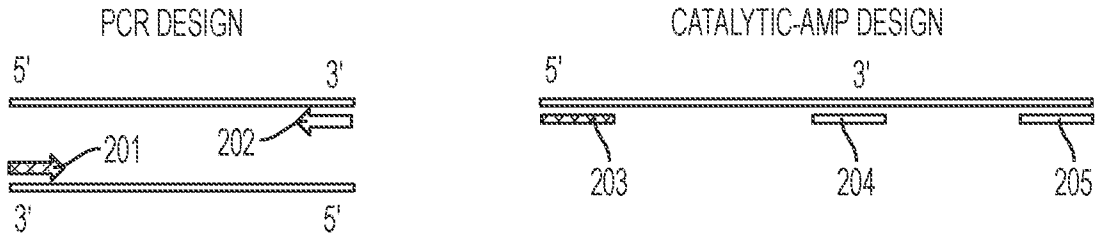


FIG. 2

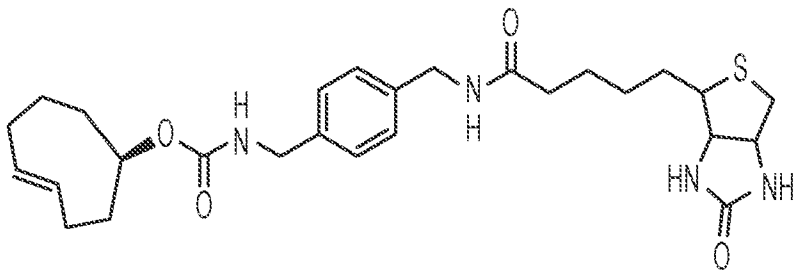


FIG. 3

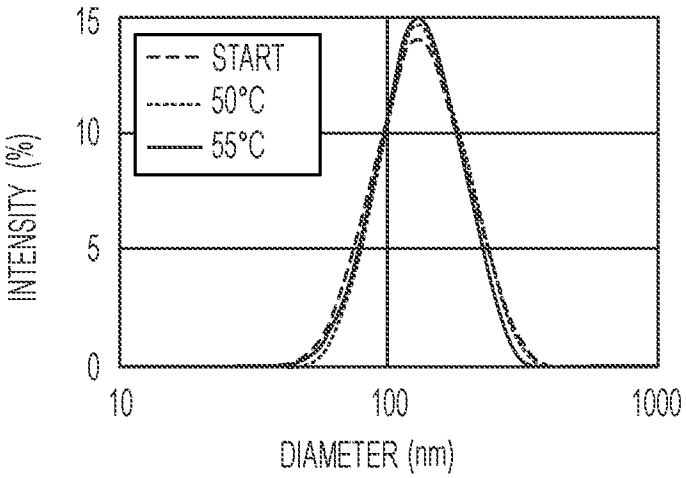


FIG. 4

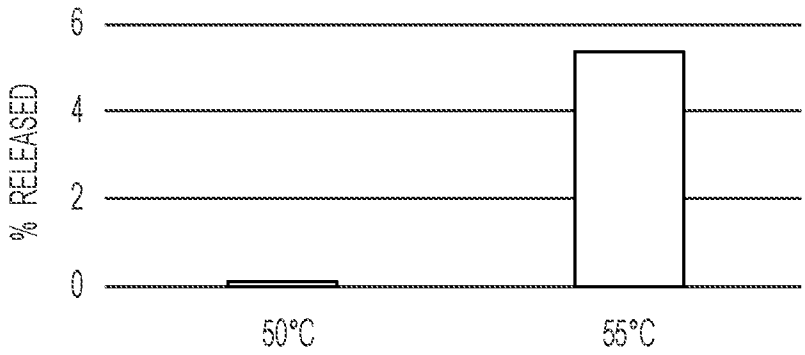


FIG. 5

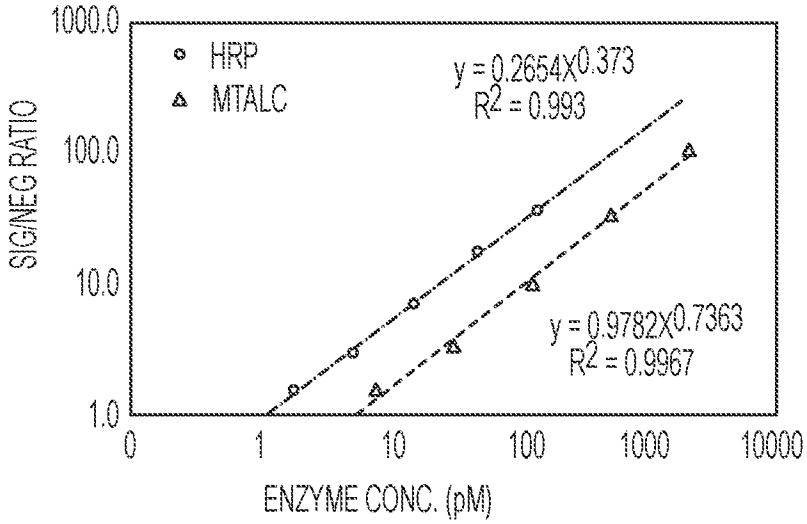

1000.0
100.0
10.0
1.0
SIG/NEG RATIO
HRP
MTALC
y = 0.2654X^0.373
R2 = 0.993
y = 0.9782X^0.7363
R2 = 0.9967
0
1
10
100
1000
10000
ENZYME CONC. (pM)

FIG. 6

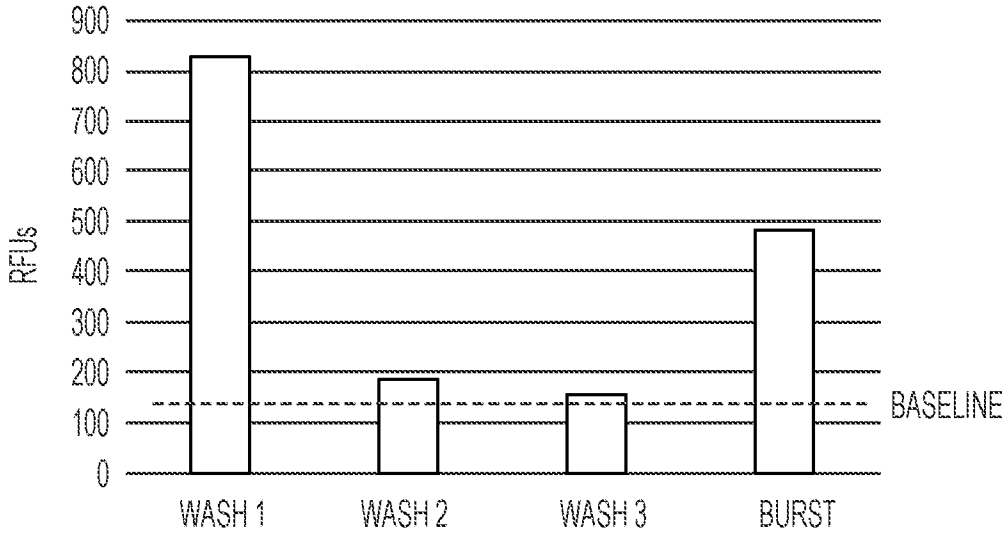

900
800
700
600
500
400
300
200
100
0
RFUs
BASELINE
WASH 1
WASH 2
WASH 3
BURST

FIG. 7

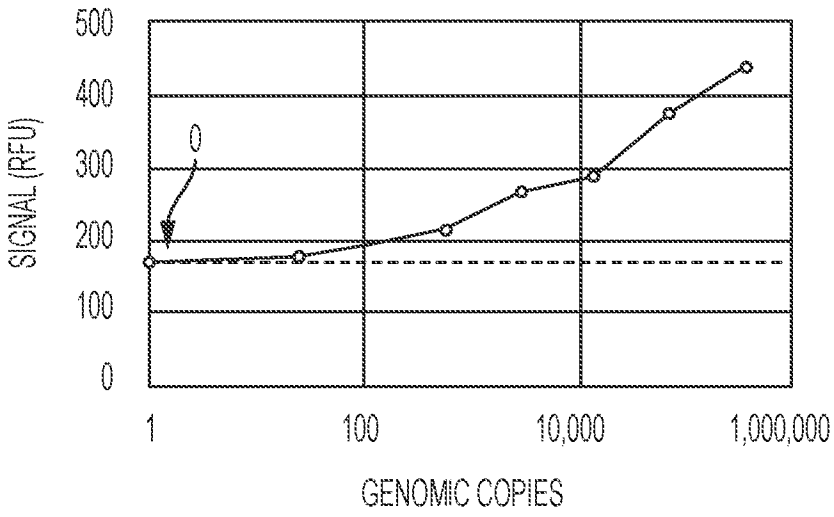

500
400
300
200
100
0
SIGNAL (RFU)
0
1
100
10,000
1,000,000
GENOMIC COPIES

FIG. 8

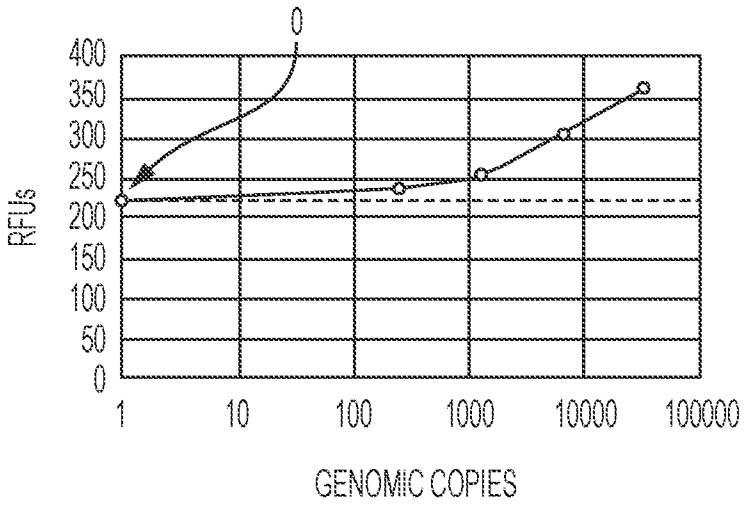

0
400
350
300
250
200
150
100
50
0
RFUs
1
10
100
1000
10000
100000
GENOMIC COPIES

FIG. 9

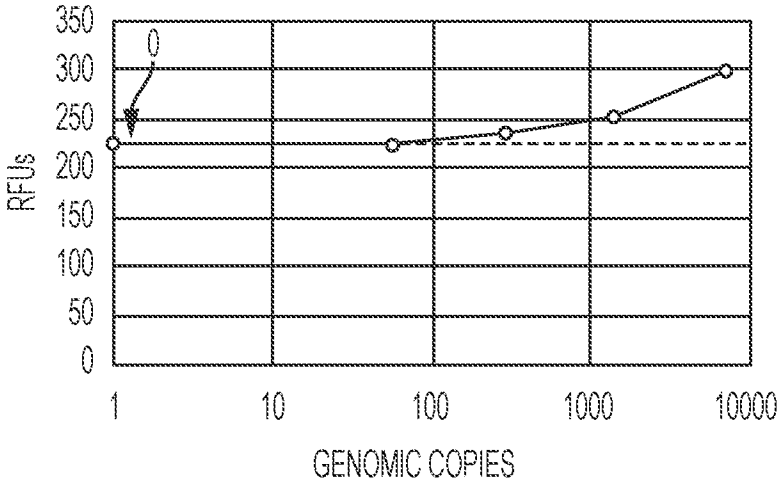

350
300
250
200
150
100
50
0
RFUs
0
1
10
100
1000
10000
GENOMIC COPIES

FIG. 10

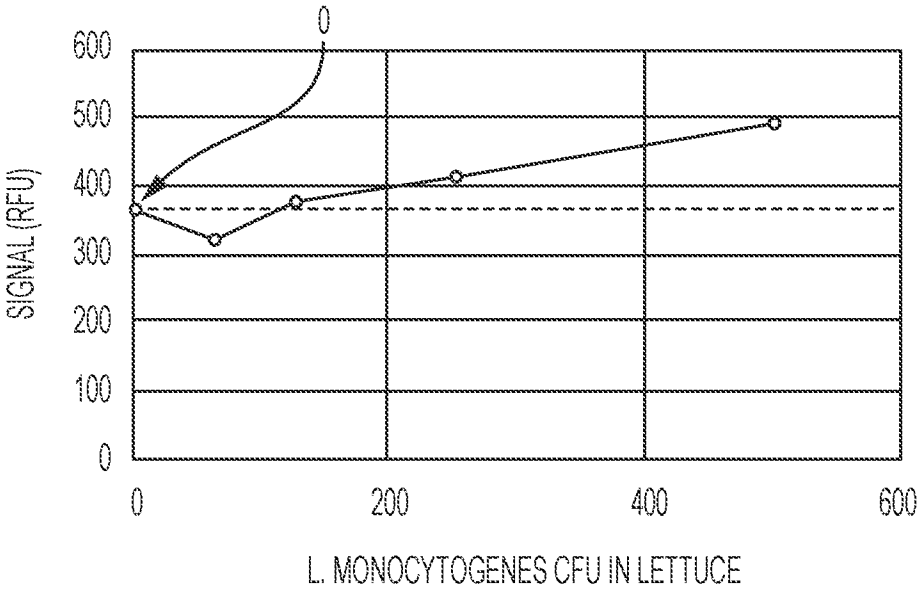

0
600
500
400
300
200
100
0
SIGNAL (RFU)
0
200
400
600
L. MONOCYTOGENES CFU IN LETTUCE

FIG. 11

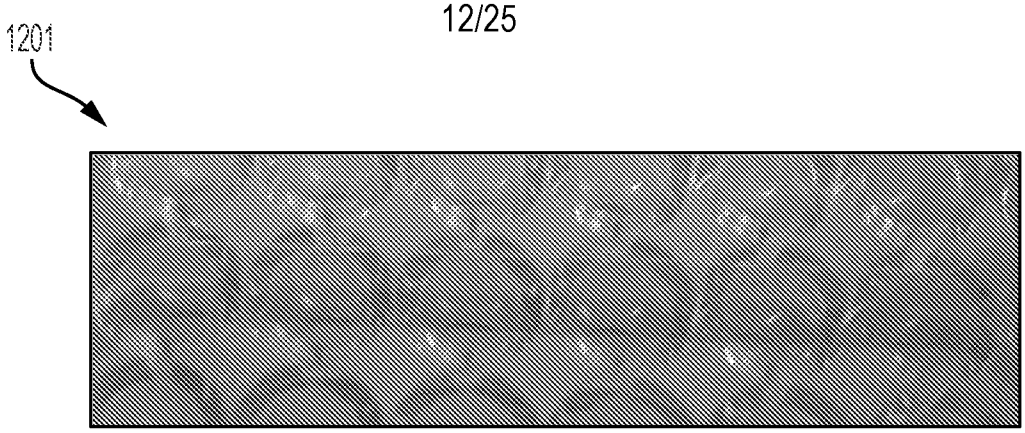


FIG. 12A

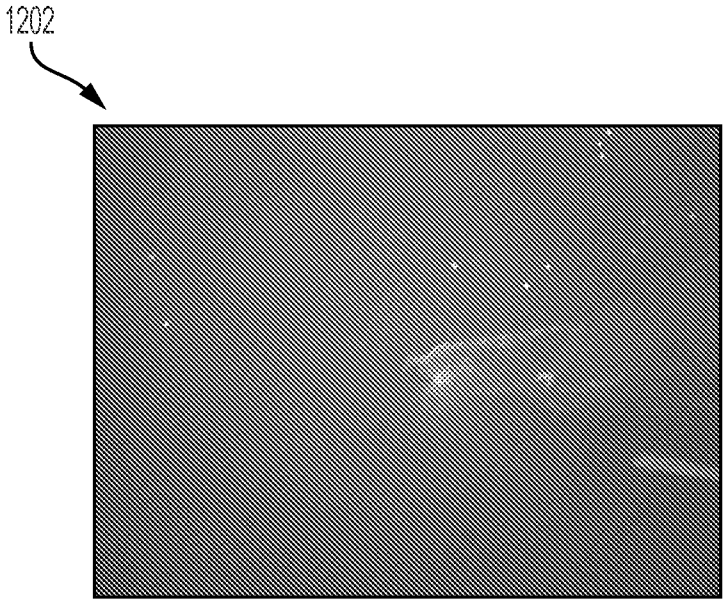


FIG. 12B

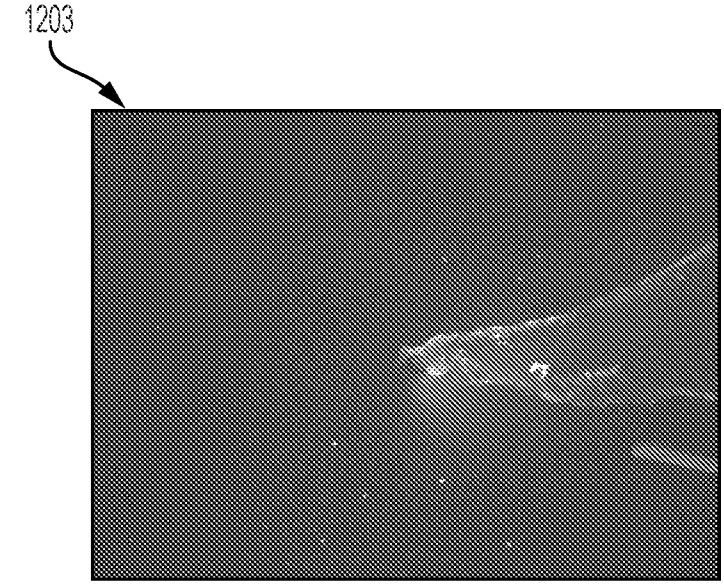


FIG. 12C

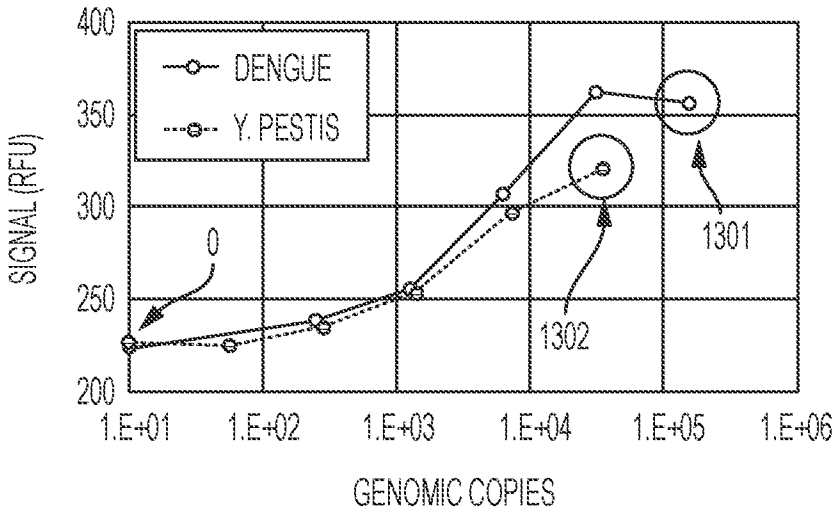

400
350
300
250
200
SIGNAL (RFU)
DENGUE
Y. PESTIS
0
1301
1302
1.E+01
1.E+02
1.E+03
1.E+04
1.E+05
1.E+06
GENOMIC COPIES

FIG. 13

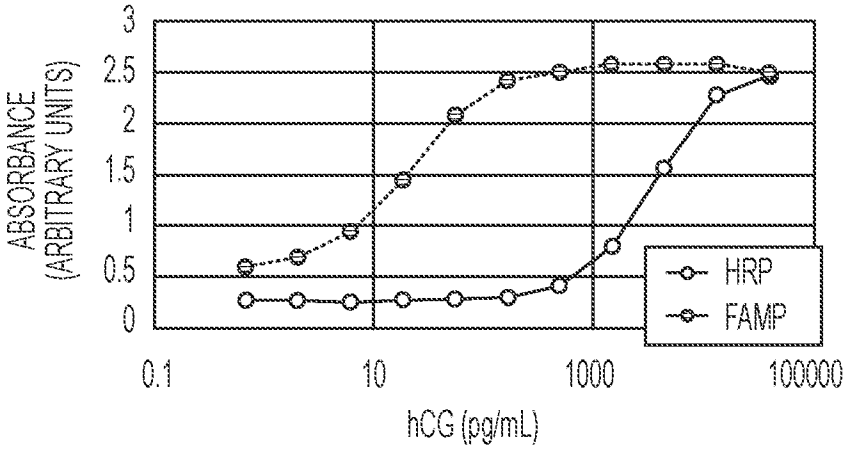

ABSORBANCE
(ARBITRARY UNITS)
3
2.5
2
1.5
1
0.5
0
0.1
10
1000
100000
hCG (pg/mL)
HRP
FAMP

FIG. 14

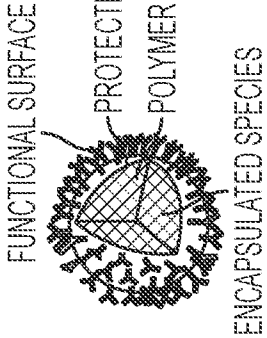
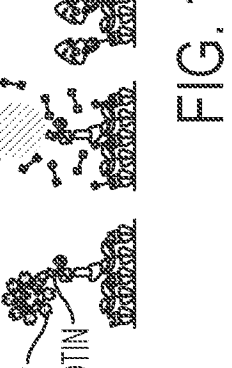


FIG. 15A



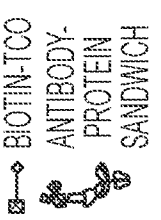


FIG. 15B

FIG. 15C

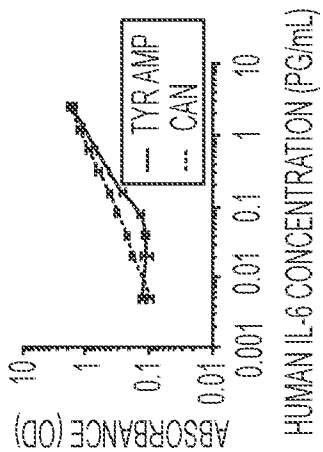


FIG. 15D

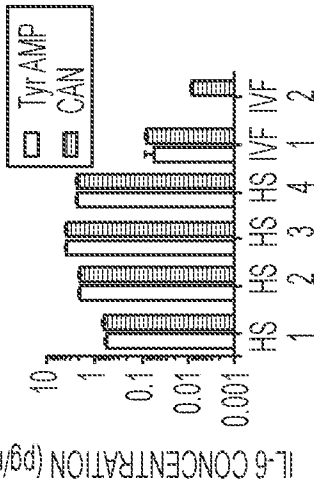


FIG. 15E

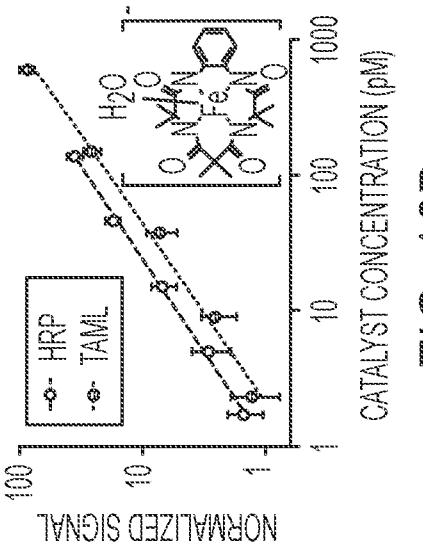


FIG. 16B

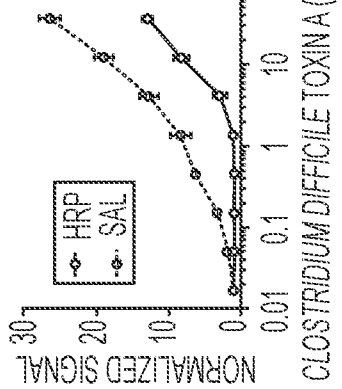


FIG. 16E

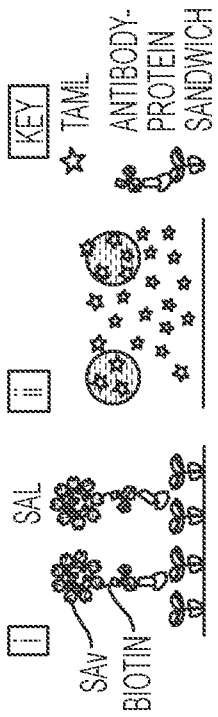


FIG. 16A

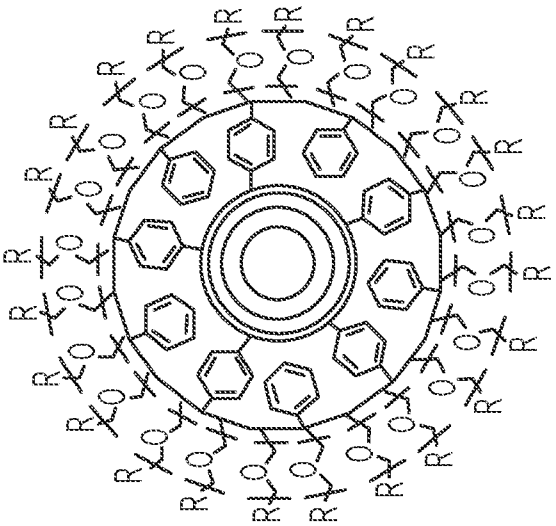


FIG. 16D

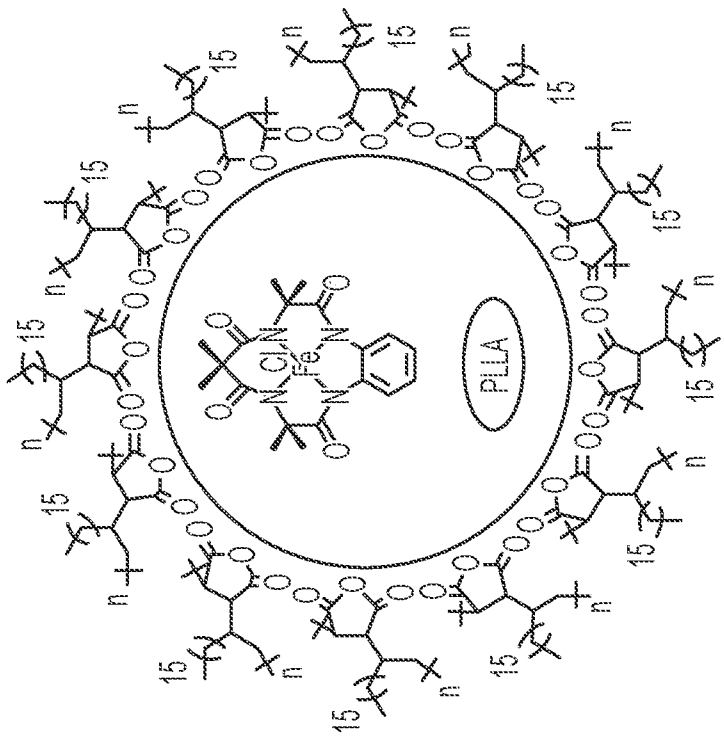


FIG. 16C

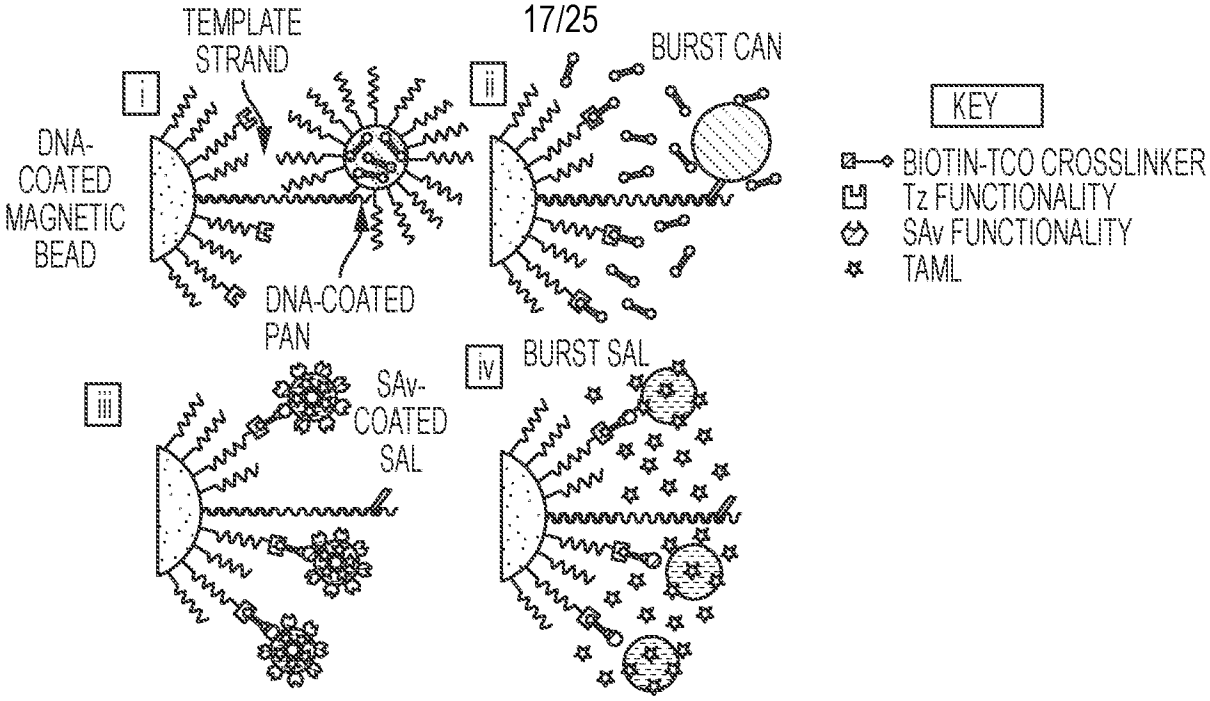


FIG. 17A

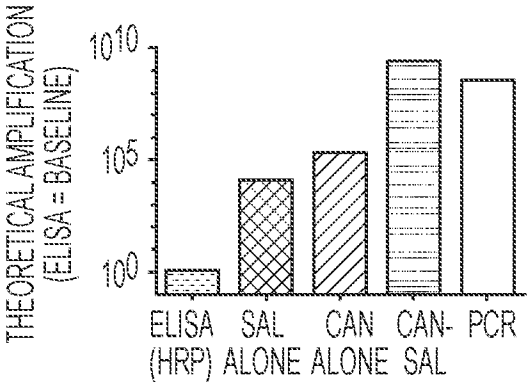


FIG. 17B

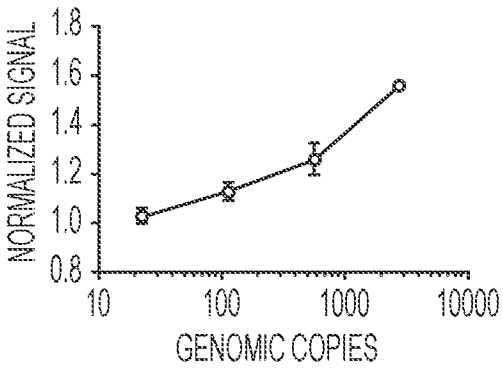


FIG. 17C

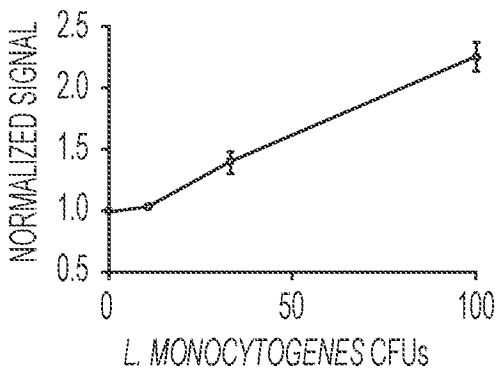


FIG. 17D

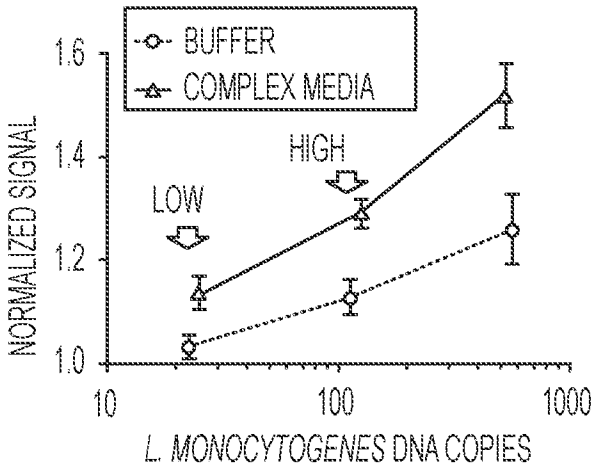


FIG. 18A

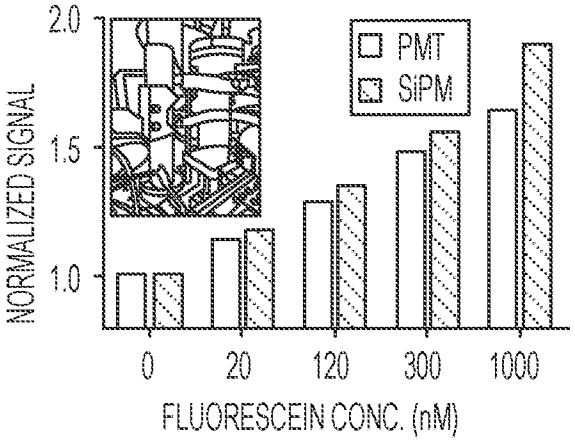


FIG. 18B

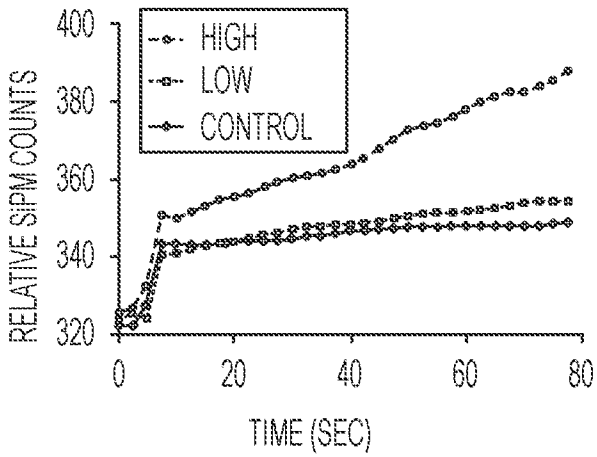


FIG. 18C

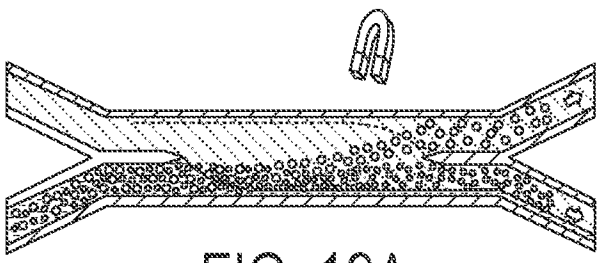


FIG. 19A

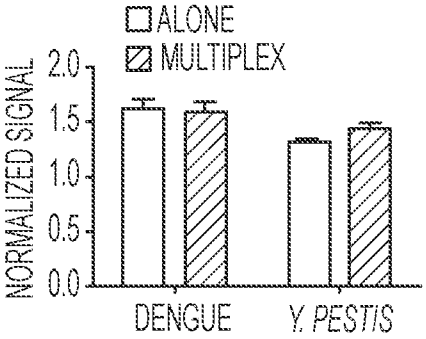


FIG. 19D

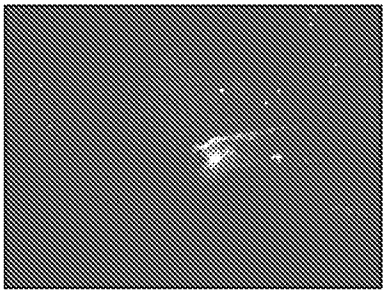


FIG. 19B

SAMPLE	PCR (rDNA/mecA)	SeLux (rRNA/mecA)
S1 (-)	- / -	- / -
S6 (-)	- / -	- / -
S2 (S. aur)	+ / -	+ / -
S5 (S. aur)	+ / -	+ / -
S3 (MRSA)	+ / +	+ / +
S4 (MRSA)	+ / +	+ / +
S7 (MRSA)	+ / +	+ / +

FIG. 19E



FIG. 19C

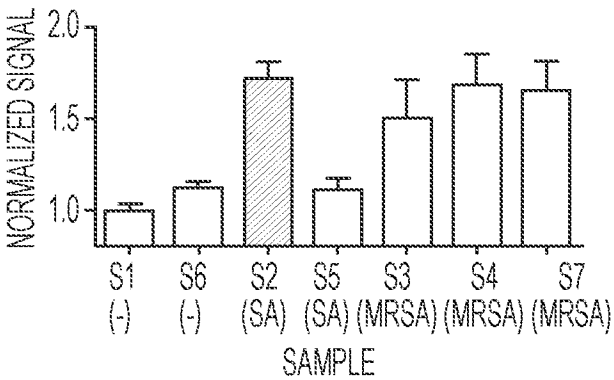


FIG. 19F

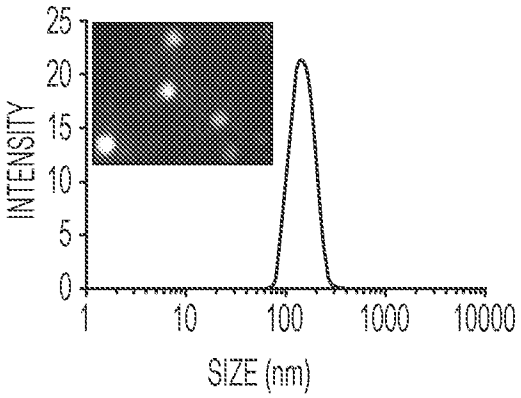


FIG. 20

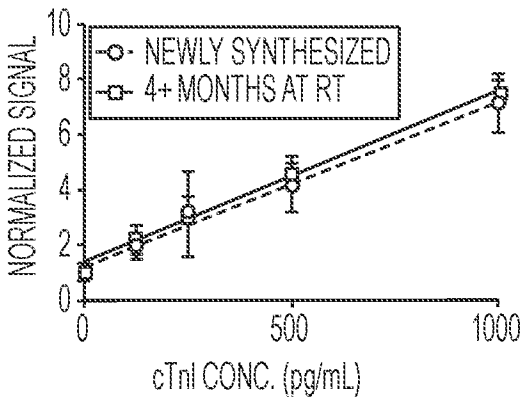

NORMALIZED SIGNAL
10
8
6
4
2
0
NEWLY SYNTHESIZED
4+ MONTHS AT RT
0
500
1000
cTnI CONC. (pg/mL)

FIG. 21

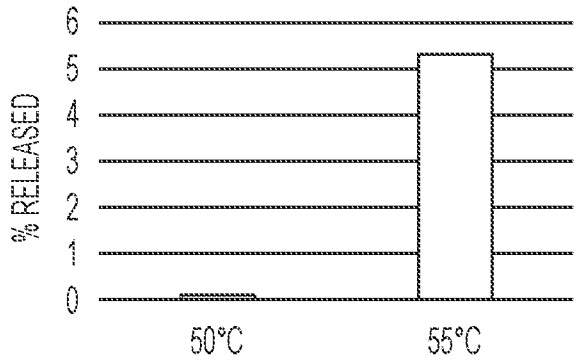


FIG. 22

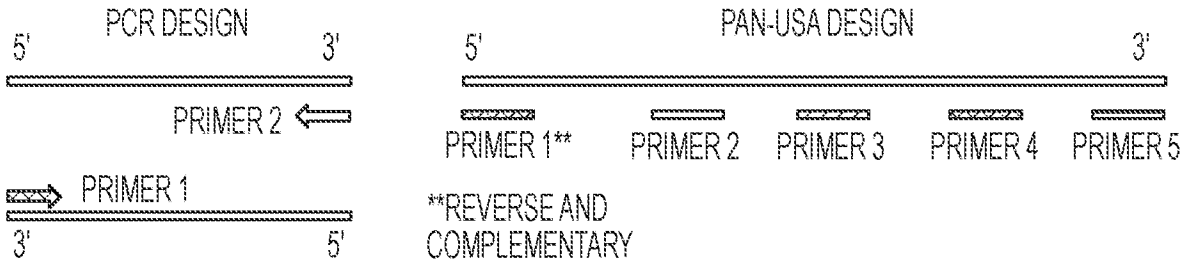

PCR DESIGN
5'
3'
PRIMER 2
PRIMER 1
3'
5'
PAN-USA DESIGN
5'
3'
PRIMER 1**
PRIMER 2
PRIMER 3
PRIMER 4
PRIMER 5
**REVERSE AND COMPLEMENTARY

FIG. 23

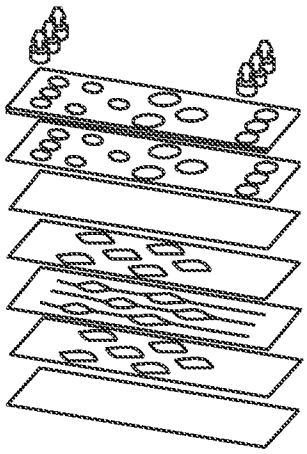


FIG. 24A

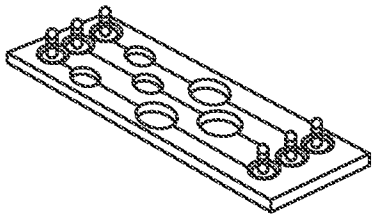


FIG. 24B

SAMPLE	PCR (rDNA/mecA)	SeLux (rRNA/mecA)
B1 (-)	- / -	- / -
B2 (-)	+ / -	+ / -
B3 (*S. aur*)	+ / -	+ / -
B4 (*S. aur*)	+ / -	+ / -
B5 (*S. aur*)	+ / -	+ / -
B6 (MRSA)	+ / +	+ / +
B7 (MRSA)	+ / +	+ / +
B8 (MRSA)	+ / +	+ / +
B9 (MRSA)	+ / +	+ / +
B10 (MRSA)	+ / +	+ / +

FIG. 25A

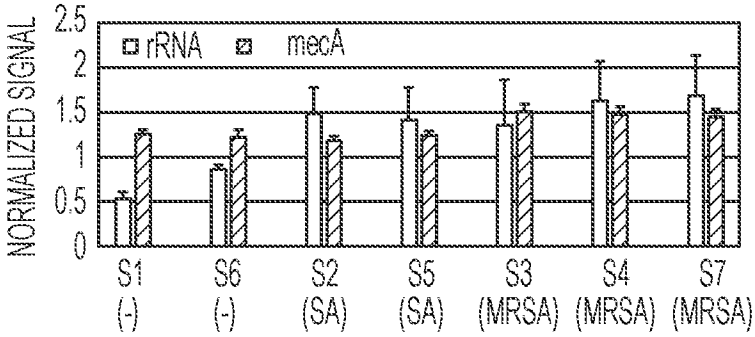


FIG. 25B

INTERNATIONAL SEARCH REPORT

International application No
PCT/US2016/065607

A. CLASSIFICATION OF SUBJECT MATTER
INV. C12Q1/68
ADD.

According to International Patent Classification (IPC) or to both national classification and IPC

B. FIELDS SEARCHED

Minimum documentation searched (classification system followed by classification symbols)
C12Q

Documentation searched other than minimum documentation to the extent that such documents are included in the fields searched

Electronic data base consulted during the international search (name of data base and, where practicable, search terms used)
EPO-Internal, BIOSIS, Sequence Search, EMBASE, WPI Data

C. DOCUMENTS CONSIDERED TO BE RELEVANT

Category*	Citation of document, with indication, where appropriate, of the relevant passages	Relevant to claim No.
X	WO 2005/062982 A2 (LI XING-XIANG [US]; WANG TIANXIN [US]) 14 July 2005 (2005-07-14) figure 11 paragraphs [0003], [0055], [0068], [0105], [0106], [0107], [0108], [0111] examples 3,7 abstract the whole document -----	1-32
A	WO 2005/085850 A1 (WANG TIANXIN [US]; LI XINGXIANG [US]) 15 September 2005 (2005-09-15) figure 5 abstract the whole document -----	1-32

-/--

[X] Further documents are listed in the continuation of Box C.

[X] See patent family annex.

* Special categories of cited documents :

"A" document defining the general state of the art which is not considered to be of particular relevance

"E" earlier application or patent but published on or after the international filing date

"L" document which may throw doubts on priority claim(s) or which is cited to establish the publication date of another citation or other special reason (as specified)

"O" document referring to an oral disclosure, use, exhibition or other means

"P" document published prior to the international filing date but later than the priority date claimed

"T" later document published after the international filing date or priority date and not in conflict with the application but cited to understand the principle or theory underlying the invention

"X" document of particular relevance; the claimed invention cannot be considered novel or cannot be considered to involve an inventive step when the document is taken alone

"Y" document of particular relevance; the claimed invention cannot be considered to involve an inventive step when the document is combined with one or more other such documents, such combination being obvious to a person skilled in the art

"&" document member of the same patent family

Date of the actual completion of the international search	Date of mailing of the international search report
14 March 2017	23/03/2017

Name and mailing address of the ISA/	Authorized officer
European Patent Office, P.B. 5818 Patentlaan 2 NL - 2280 HV Rijswijk Tel. (+31-70) 340-2040, Fax: (+31-70) 340-3016	Helliot, Bertrand

INTERNATIONAL SEARCH REPORT

International application No
PCT/US2016/065607

C(Continuation). DOCUMENTS CONSIDERED TO BE RELEVANT

Category*	Citation of document, with indication, where appropriate, of the relevant passages	Relevant to claim No.
A	WO 03/104424 A2 (US GOV HEALTH & HUMAN SERV [US]; DHAWAN SUBHASH [US]) 18 December 2003 (2003-12-18) figure 1 abstract the whole document -----	1-32

INTERNATIONAL SEARCH REPORT

Information on patent family members

International application No
PCT/US2016/065607

Patent document cited in search report	Publication date	Patent family member(s)	Publication date
WO 2005062982 A2	14-07-2005	NONE	
WO 2005085850 A1	15-09-2005	US 2005191687 A1	01-09-2005
		WO 2005085850 A1	15-09-2005
WO 03104424 A2	18-12-2003	AU 2003251428 A1	22-12-2003
		WO 03104424 A2	18-12-2003